

PRELIMINARY INVESTIGATION AND PROTOCOL DEVELOPMENT FOR  
*IN VITRO* OPTICALLY STIMULATED LUMINESCENT DOSIMETRY OF  
MULTIPLE INTRABEAM® APPLICATORS IN A CANINE TISSUE MODEL

By

Tyler Roberts

A THESIS

Presented to the Department of Medical Physics

and the Oregon Health & Science University

School of Medicine

in partial fulfillment of

the requirements for the degree of

Master of Science

June 2018

School of Medicine

Oregon Health & Science University

---

CERTIFICATE OF APPROVAL

---

This is to certify that the Master's thesis of

Tyler Roberts

has been approved

---

Mentor/Advisor – Krystina Tack

---

Member – Susha Pillai

---

Member – Thomas Griglock

©Copyright by Tyler Roberts  
June 2018  
All Rights Reserved

# Table of Contents

|  |     |
|--|-----|
| List of Figures .....  | iii |
| List of Tables.....  | iv  |
| Acknowledgements .....   | v   |
| Abstract.....  | vi  |
| 1. Introduction.....   | 1   |
| 2. Background and Materials .....                              | 2   |
| 2.1. Cancer Treatment in Veterinary Medicine.....              | 2   |
| 2.2. Intrabeam.....  | 2   |
| 2.2.1. Device Description .....                                | 2   |
| 2.2.2. Applicators.....  | 5   |
| 2.2.3. Energy Spectrum .....                                   | 8   |
| 2.3. Intrabeam Dose Rate and Isotropy Measurement.....         | 9   |
| 2.3.1. Intrabeam Water Phantom .....                           | 9   |
| 2.3.2. Soft X-Ray Chamber .....                                | 11  |
| 2.4. Dosimetric Measurements with OSLDs .....                  | 12  |
| 2.4.1. Landauer nanoDots.....                                  | 12  |
| 2.4.2. Optically Stimulated Luminescence .....                 | 13  |
| 2.4.3. Energy Response .....                                   | 13  |
| 2.4.4. microStar Reader and Calibration.....                   | 14  |
| 3. Methods .....   | 16  |
| 3.1. Applicator, Prescription, and Depth Selections .....      | 16  |
| 3.2. 3D Printed nanoDot Holder.....                            | 17  |
| 3.3. Measurement of Dose Rate with Ion Chamber in Water .....  | 19  |
| 3.4. Point Calibration of OSLDs in Water Tank .....            | 20  |
| 3.5. Harvesting Tissue for Measurement .....                   | 23  |
| 3.6. Imaging of Tissue.....                                    | 24  |
| 3.7. Irradiation of Tissue.....                                | 25  |
| 4. Results .....   | 26  |
| 4.1. Ion Chamber Measurements.....                             | 26  |
| 4.2. nanoDot Measurements in the Intrabeam Water Phantom ..... | 28  |

|        |   |    |
|--------|---|----|
| 4.3.   | Harvested Tissue .....  | 30 |
| 4.3.1. | CT Measurements .....   | 30 |
| 4.4.   | <i>in vitro</i> Measurements.....                               | 30 |
| 4.5.   | Protocol.....   | 31 |
| 5.     | Discussion .....  | 32 |
| 5.1.   | Ion Chamber Measurements.....                                   | 32 |
| 5.2.   | nanoDot Measurements in the Intrabeam Water Phantom .....       | 32 |
| 5.3.   | Harvested Tissue .....  | 33 |
| 5.4.   | <i>in vitro</i> Measurements.....                               | 34 |
| 5.5.   | Sources of Variability and Recommended Protocol .....           | 34 |
| 6.     | Future Directions .....   | 35 |
| 7.     | Conclusion .....  | 36 |
| 8.     | References .....  | 37 |
| 9.     | Appendix .....  | 41 |
| A.     | Suggested Protocol for Intrabeam OSL Dosimetric Assessment..... | 41 |
| B.     | Sample Data Tables .....  | 48 |

# List of Figures

|   |           |
|---|-----------|
| <b>Figure 1. The Intrabeam PRS 500 and articulating arm.....</b>                      | <b>3</b>  |
| <b>Figure 2. The PDA and PAICH .....</b>  | <b>4</b>  |
| <b>Figure 3. The spherical applicator and its dose distribution.....</b>              | <b>5</b>  |
| <b>Figure 4. The flat applicator and its dose distribution.....</b>                   | <b>6</b>  |
| <b>Figure 5. The surface applicator and its dose distribution .....</b>               | <b>7</b>  |
| <b>Figure 6. Dose rate as a function of depth for each applicator.....</b>            | <b>7</b>  |
| <b>Figure 7. The spectrum of the Intrabeam XRS at depth.....</b>                      | <b>8</b>  |
| <b>Figure 8. Water Phantom and Ion Chamber .....</b>                                  | <b>9</b>  |
| <b>Figure 9. Spherical Applicator in Water Tank.....</b>                              | <b>10</b> |
| <b>Figure 10. Landauer nanoDot.....</b>   | <b>12</b> |
| <b>Figure 11. OSLD Response.....</b>  | <b>14</b> |
| <b>Figure 12. 3D Printer nanoDot Holder.....</b>                                      | <b>18</b> |
| <b>Figure 13. CT of nanoDot Holder.....</b>   | <b>19</b> |
| <b>Figure 14. IntraBeam QA with P&amp;T Correction Factor and Output Factor .....</b> | <b>20</b> |
| <b>Figure 15. Shift for difference in measurement point .....</b>                     | <b>21</b> |
| <b>Figure 16. Entering a Prescription Dose.....</b>                                   | <b>22</b> |
| <b>Figure 17. Tissue Samples Immediately After Harvesting.....</b>                    | <b>23</b> |
| <b>Figure 18. Tissue on Plastic Water before CT.....</b>                              | <b>24</b> |
| <b>Figure 19. nanoDot Placed for Measurement.....</b>                                 | <b>25</b> |
| <b>Figure 20. Flat Applicator on Tissue .....</b>                                     | <b>26</b> |
| <b>Figure 21. Response in Counts per cGy by Applicator .....</b>                      | <b>29</b> |
| <b>Figure 22. Tissue CTs.....</b>   | <b>30</b> |
| <b>Figure 23. Early Treatment Termination.....</b>                                    | <b>44</b> |
| <b>Figure 24. nanoDot Orientation in Holder .....</b>                                 | <b>44</b> |
| <b>Figure 25. Tissue Slab Diagram.....</b>  | <b>45</b> |
| <b>Figure 26. nanoDot Placement on Bolus .....</b>                                    | <b>46</b> |
| <b>Figure 27. Applicator Placement on Tissue .....</b>                                | <b>47</b> |

# List of Tables

|  |           |
|--|-----------|
| <b>Table 1. Ion Chamber Results .....</b>                            | <b>28</b> |
| <b>Table 2. Preliminary nanoDot Water Tank Results .....</b>         | <b>29</b> |
| <b>Table 3. Preliminary Counts at Depth in Tissue .....</b>          | <b>31</b> |
| <b>Table 4. Preliminary Counts in Tissue Relative to Water .....</b> | <b>31</b> |
| <b>Table 5. Sources of Variability and Potential Solutions .....</b> | <b>35</b> |
| <b>Table 6. Sample Data Table for nanoDot Calibrations.....</b>      | <b>48</b> |
| <b>Table 7. Sample Data Table for Water Tank Measurements .....</b>  | <b>49</b> |
| <b>Table 8. Sample Data Table for Tissue Measurements.....</b>       | <b>49</b> |

## Acknowledgements

I would like to express immense appreciation to the faculty at OHSU for their indelible role in my education. A tremendous gratitude to Dr. Krystina Tack's willingness to add me to her busy schedule when I needed a new thesis project at the last minute. Your encouragement when I felt anything but was invaluable. To Susha Pillai and Dr. Thomas Griglock for their ears and insights during my research, a debt is owed. Thank you to Elizabeth Shiner, Shay Bracha, and Milan Milovancev. Your generosity with your time especially in the face of injuries and new additions was above and beyond.

To the members of the staff and faculty in Radiation Medicine who have made me feel at home since the day I stepped foot in this department: Thanks to all of you. Thank you to all those that have shared an office with me: my fellow students, Tom & MacKenzie; Ramtin; Jessie; and Celeste. You've made these days easier.

Thank you to my mother, my family, and all of the rest of my *extensive* extended family for making me so at home here in Portland. To my wife, Mitra, I owe everything. I would never have made this circuitous route to where I am today without you. Thank you for being there with me every step of the way. The support I have received from you and your family have been paramount.

# Abstract

## Background:

The IntraBeam (Zeiss) intraoperative radiotherapy (IORT) device has been in wide use in the treatment of human cancers in the brain, breast, and other sites for more than a decade, but its use in Veterinary Medicine has thus far been exclusive to Oregon State University (OSU). OHSU and OSU have set about to do a dosimetric assessment on the IntraBeam as it relates to animal tissues. Optically Stimulated Luminescent Dosimeters (OSLDs) are commonly used for *in vivo* dosimetry for their small, radiolucent package and relative accuracy. However, their varying energy response in the kilovoltage range of the IntraBeam (50 kVp) makes their use in precise dosimetry more difficult, particularly when making measurements at varying depths where beam hardening effects will cause varied response between depths. The microStar reader used in conjunction with nanoDots allows for multiple calibrations that can be used for the various applicators (spherical, surface, and flat) and depths relevant to an IntraBeam treatment. The purpose of this study was to make preliminary measurements in the Zeiss Water Phantom and in tissue in order to derive a protocol that would facilitate repeatable tissue measurements across multiple tissue types in the future.

## Methods:

Measurements were made to determine dose rate at depth (Gy/min) with an ionization chamber in the Zeiss Water Phantom. These values were then used to create a point calibration at each depth using nanoDots and 1 to 2 prescription doses. Point calibrations were performed instead of complete calibrations in the interest of time. Homogeneous canine muscle tissue samples were obtained at thicknesses corresponding to the depths measured in water. The tissue samples were irradiated with nanoDots beneath.

**Results:**

Point calibrations proved to be an unreliable method. The values obtained from nanoDots did not show a meaningful trend. The tissue samples obtained had thicknesses that greatly varied from the desired thicknesses. This made analysis of the dose in tissue compared to in water impossible. The experiences encountered in carrying out these methods were analyzed to determine places for improvement, and a protocol was derived. The protocol included a method for carrying out calibrations across multiple depths with additional dose levels per calibration. A method to create more precise and repeatable tissue samples was devised along with revised recommendations for tissue thicknesses.

**Conclusion:**

Preliminary measurements were carried out in order to derive a protocol for measurement in tissues. The protocol was derived and will allow for a dosimetric assessment of the Intrabeam to be performed with nanoDots in a canine tissue model regardless of tissue type.

# 1. Introduction

Oregon State University's Carlson College of Veterinary Medicine (OSU) has used the Zeiss Intrabeam® to perform intraoperative radiation therapy (IORT) on animals including dogs, cats, and horses, since 2014. Many of these cases have a positive outcome, but to this point, there has not been a dosimetric assessment of the unique anatomy in veterinary medicine with respect to Intrabeam. It is hypothesized that the nanoDot™ optically stimulated luminescent dosimeter (OSLD) by Landauer® can be used to assess the dose from the Intrabeam in water phantoms and in *in vitro* situations using tissue samples from areas frequently treated for cancer in veterinary medicine. This thesis will provide a description of a number of steps undertaken for preliminary measurements and establish a protocol for the dosimetric assessment described above in a canine model.

The Intrabeam operates at an energy of 50 kV using a miniaturized linear accelerator and a variety of applicators that can provide dose distributions that are flat at depth, high at the surface, or spherical in shape. At this energy, however, nanoDots exhibit a highly non-linear energy dependence [1]–[3]. Coupled with beam hardening that occurs rapidly with depth at the kilovoltage range, OSLD response should vary with depth [4]. To the author's knowledge an investigation of and calibration of OSLDs at specific depths with Intrabeam has not been performed, so one of the aims of the above protocol is to establish a calibration procedure for multiple depths.

The thesis will describe the methods undertaken for preliminary measurements and offers a protocol based on the experiences and findings during the preliminary measurements. The preliminary measurements and protocol will describe how steps for measuring homogeneous muscle tissue. Future directions will indicate recommended measurements in alternative tissues and full cadavers.

## **2. Background and Materials**

### **2.1. Cancer Treatment in Veterinary Medicine**

Small animal veterinary patients suffer from many of the same tumor types as humans, with notable similarities between the species in terms of tumor biology and treatment options. This includes the broad category of soft tissue sarcoma as well as head and neck tumors such as oral squamous cell carcinoma and melanoma [5]–[8]. Standard of care for many of these tumor types in veterinary species includes surgical resection with wide margins in an attempt to obtain histologically complete excision [7], [9]. In cases where wide excision is not possible, adjuvant post-operative external beam radiation therapy has been shown to improve clinical outcomes [7], [10], [11]. However, the financial costs, availability, logistical challenges, and need for general anesthesia in animal patients presents challenges to delivery of external beam radiation therapy for these veterinary patients.

In humans with early mammary carcinoma, a single dose of targeted intraoperative radiotherapy has been shown to be an effective alternative to external beam radiotherapy delivered over several weeks [12]. To the author's knowledge, there are no peer-reviewed publications describing the use of targeted intraoperative radiotherapy in veterinary patients.

### **2.2. Intrabeam**

#### **2.2.1. Device Description**

The Intrabeam (Carl Zeiss) is a kilovoltage IORT device that can be equipped to with various applicators to optimize its dose distribution for treatments in the breast, brain, skin, and GI, among others [13]. The Intrabeam uses a miniature linear accelerator to create photons at 40 or 50 kVp. The increase in Relative Biological Effectiveness (RBE) of radiation

at this energy due to high ionization density along with rapid dose gradient make it an appealing option for treatment [14].



**Figure 1. The Intrabeam PRS 500 and articulating arm.**

The X-Ray Source (XRS) is equipped with an internal radiation monitor (IRM) that operates when the device is in operation to verify that the radiation output is within tolerance values by comparing the number of backscattered photons, which is proportional to the photon output [15]. The accelerator section increases the energy of the electrons produced by the cathode gun to the desired peak voltage [13]. The beam deflector steers the electrons down the probe tip which is shielded from magnetic fields [16]. A 2 cm length of 0.5 mm thick beryllium at the end of the probe tip houses a 1  $\mu\text{m}$  thick gold target which produces photons

at 40 or 50 kVp (HVL 0.64 mm Al at 10 mm depth in water) in a spherical distribution [13], [16], [17].

The Intrabeam system uses a set of quality assurance (QA) tools to ensure satisfactory performance before all treatments. The tools included fit around the XRS and check alignment, steering, isotropy and IRM, and output. The QA processes is required within 36 hours of a treatment and must be repeated after three successive treatments of the same patient or for treatment of a new patient [15]. Mandatory QA for each patient includes the isotropy and IRM and output measurements. If either of these fails QA, the physical alignment of the probe is checked, and dynamic offsets with the beam deflectors is performed [15]. The output measurements, measured with an ionization chamber, and the IRM are used to set treatment times by measuring the dose output in air relative to output at calibration and to monitor the output during treatment, respectively. If the treatment time is exceeded by 10% and the IRM has not detected enough radiation, the treatment will terminate [15].

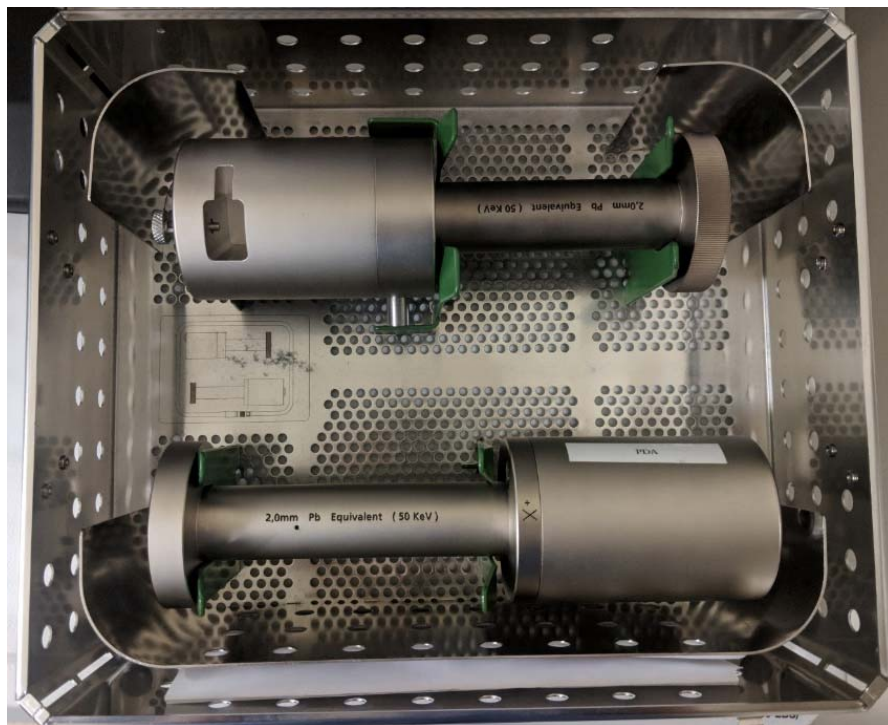


**Figure 2. The PDA and PAICH**

### 2.2.2. Applicators

The Intrabeam can be used with the XRS covered by a thin stainless-steel needle to treat brain and spine tumors or in combination with three different applicator types (Fig. 3-5). The spherical applicator creates a spherical dose distribution like the bare XRS. The flat applicator creates a flat dose distribution at 5 mm depth. The surface applicator creates a flat dose distribution at the applicator surface [13]. With the exception of the needle, all applicators come in a variety of sizes depending on the specific treatment. The spherical applicator is currently in use at OSU with the flat and surface applicators intended for use.

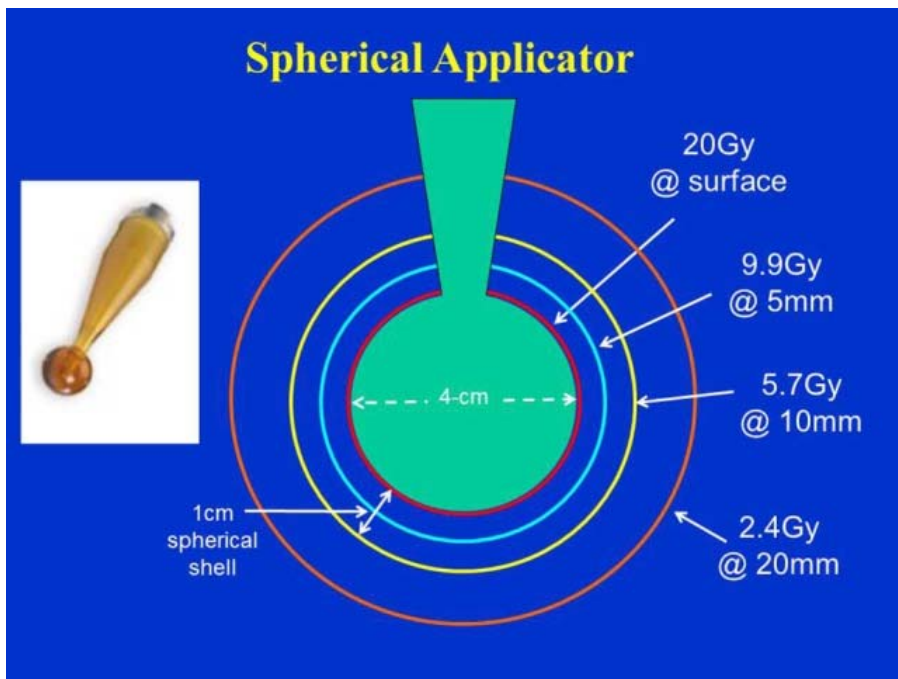


**Figure 3. The spherical applicator and its dose distribution.**

**Copyright© - Sethi, Emami, Small and Thomas with CC-BY. [10.3389/fonc.2018.00074](https://doi.org/10.3389/fonc.2018.00074)**

Due to their varied geometries and dose distributions each applicator has a different depth dose curve. Figure 6 shows a representative depth dose curve from each of the three applicator types used at OSU. These curves along with the dose distributions in figures 3-5 illustrate the suitability for each applicator to its intended purpose. The spherical applicator

is ideal for treating the tumor bed in a cavity after surgical removal of a tumor in the brain or breast, as it is commonly used in humans [12]. The flat applicator is suited for treating the tumor bed of excised GI tumors. The surface applicator is used to treat non-melanoma skin cancers [13].

Each applicator used a thermoplastic polyetherimide to achieve their dose distribution [18]. The probe tip is located at the center of the spherical applicators, while it ranges between 9.6-21.6 and 9.6-25.6 mm from the exterior of the surface and flat applicators, respectively [18]. The polyetherimide acts as a flattening filter in both the surface (2.7-5.4 mm thick) and flat (7.0-23.5 mm thick) applicators [18]. This difference in thickness creates the character distributions with flatness at different depths between the two applicator types. The flat and surface applicators are enveloped in a 0.05 mm lead equivalent shield to each side, so that dose is directed downward only [18].

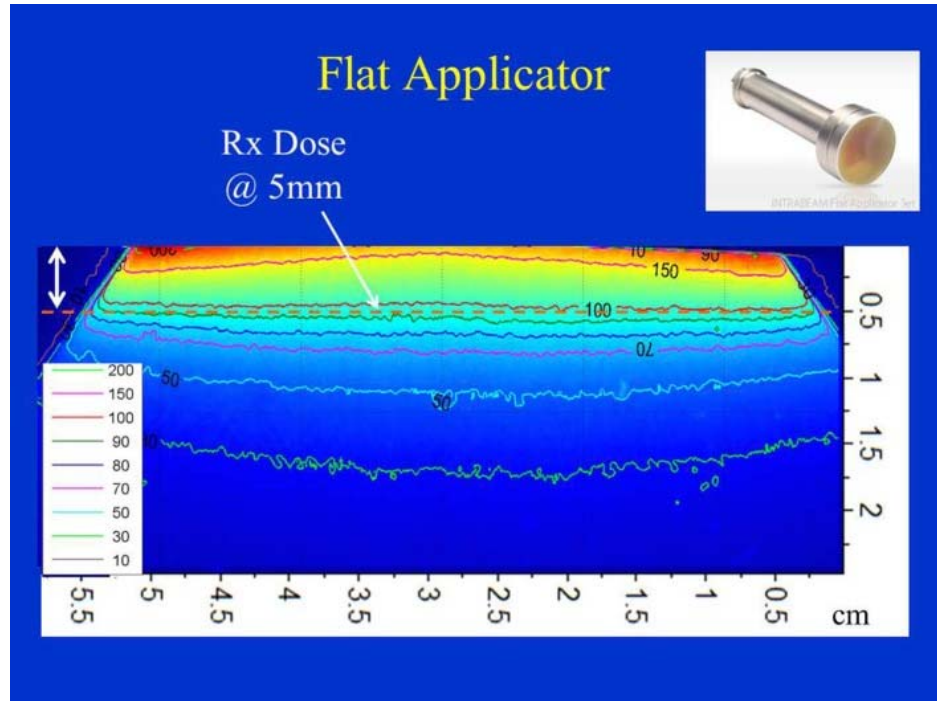


**Figure 4. The flat applicator and its dose distribution**

Copyright© - Sethi, Emami, Small and Thomas with CC-BY. [10.3389/fonc.2018.00074](https://doi.org/10.3389/fonc.2018.00074)

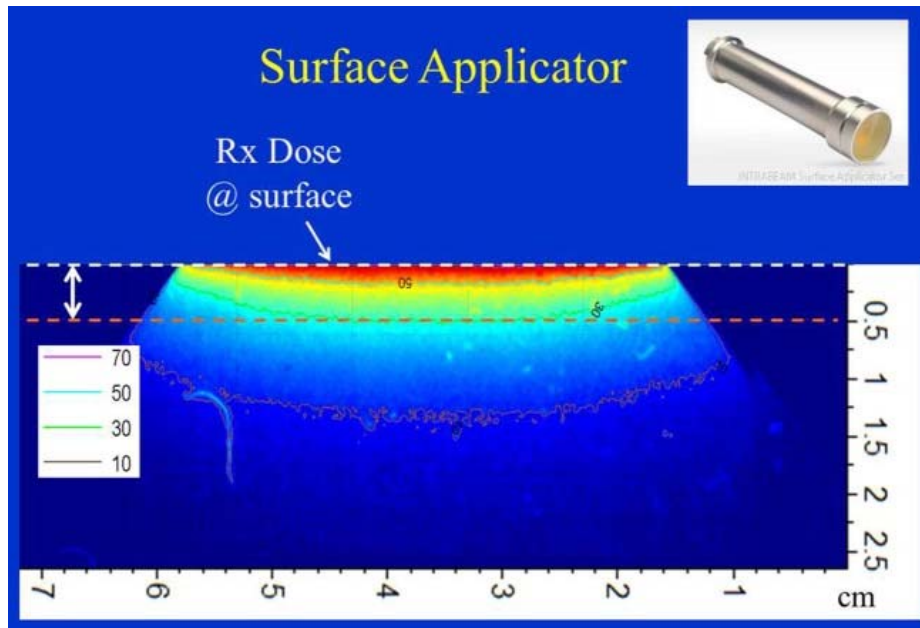


Figure 5. The surface applicator and its dose distribution

Copyright© – Sethi, Emami, Small and Thomas with CC-BY. [10.3389/fonc.2018.00074](https://doi.org/10.3389/fonc.2018.00074)

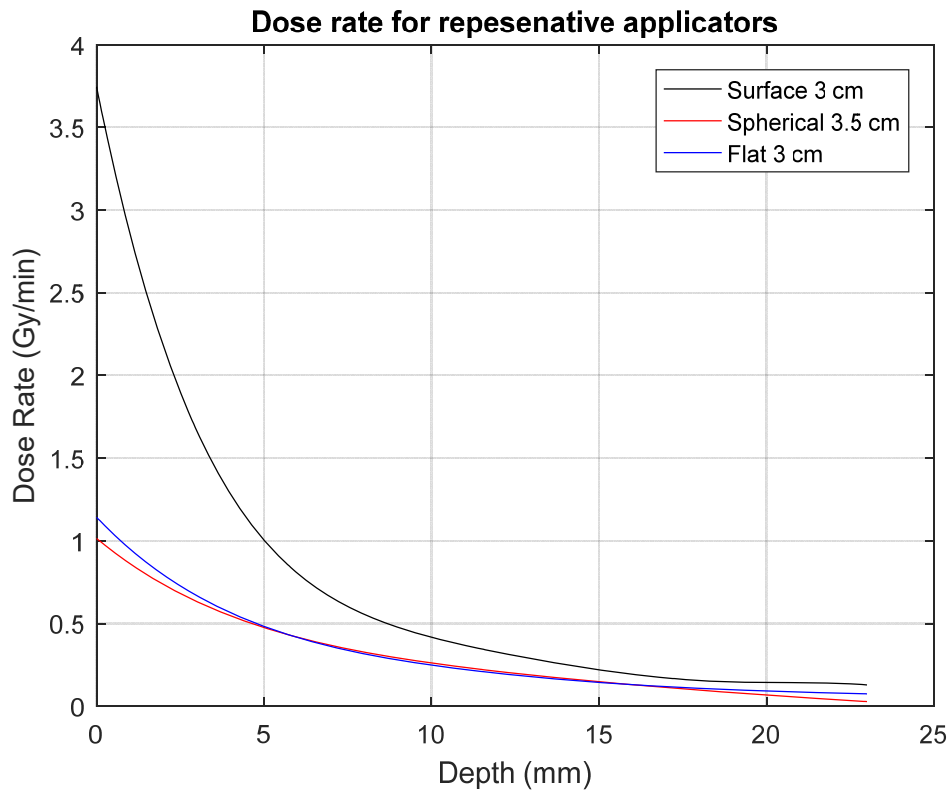


Figure 6. Dose rate as a function of depth for each applicator.

### 2.2.3. Energy Spectrum

The energy spectrum of the Intrabeam is constrained by the peak voltage at which the accelerator is driven (i.e. 40 or 50 kV). Its gold target has L-lines at 9.7, 11.5, and 13.4 keV [19]. However, with filtration provided by the applicators, these lines do not contribute to dose Spectroscopy has been performed at various depths to show the change in spectrum with depth. Beam hardening, which is caused by lower energy photons being attenuated more quickly with depth than higher energy photons, causes the mean energy to increase with depth. For the XRS in water, the mean energy at depths of 0, 5, 15, and 30 mm is 19.5, 27.3, 31.5, and 34 keV, respectively [4]. As energy response is an important quantity to consider when measuring dose, this change in beam quality must be considered for a dosimetric assessment [20].

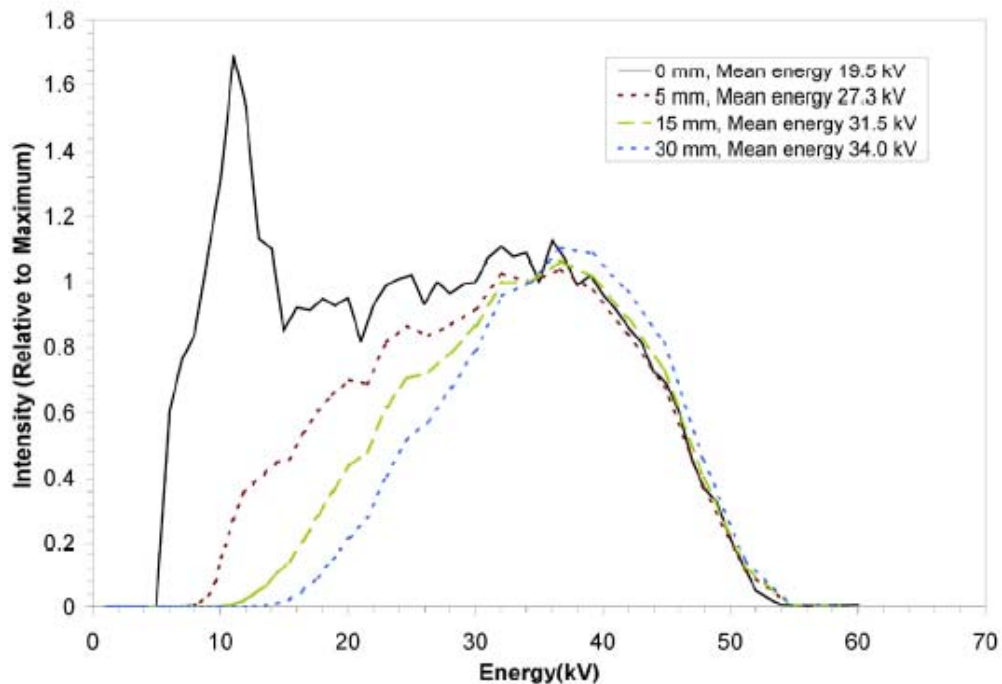


Figure 7. The spectrum of the Intrabeam XRS at depth.

Copyright © Ebert, Asad, Siddiqui with CC-BY.  
<https://doi.org/10.1120/jacmp.v10i4.2957>

## 2.3. Intrabeam Dose Rate and Isotropy Measurement

### 2.3.1. Intrabeam Water Phantom

The Intrabeam Water Phantom (Fig. 8) is used for characterizing the operation of the Intrabeam system and is described fully in the "INTRABEAM® Water Phantom – Instructions for Use" which can be referred to for more details on the remainder of this section[17]. The water tank is fully-shielded and mounts the Intrabeam repeatably with pins. It is used to measure the dose rate and depth dose curve as well as the isotropy of the Intrabeam. Any applicator can be mounted so that the dosimetric characteristics of the bare XRS and all applicators can be assessed.

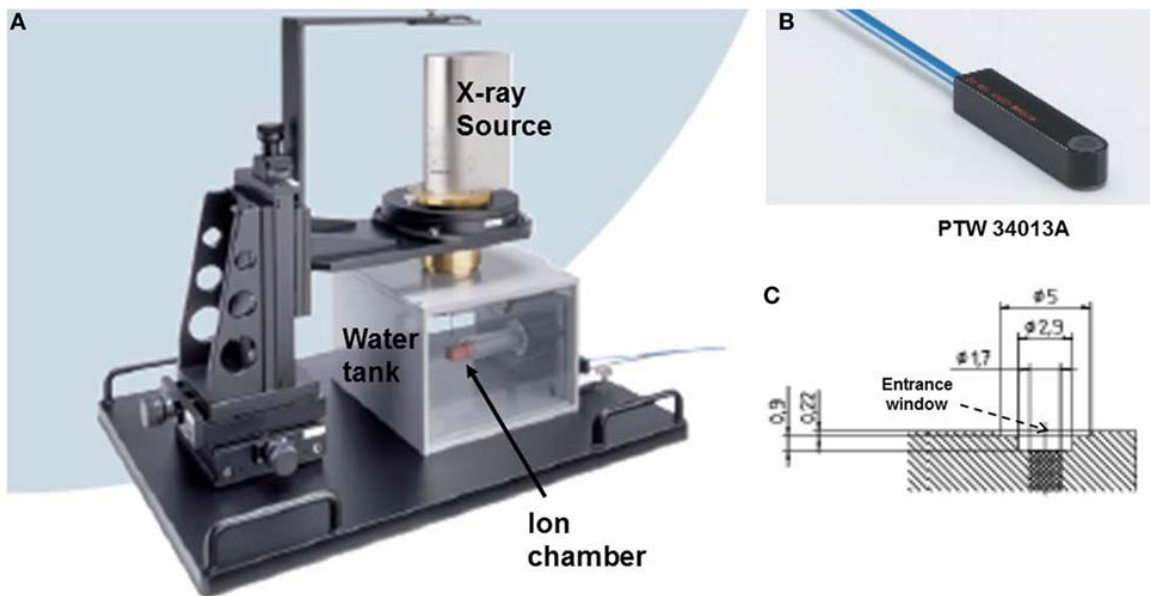


**Figure 8. Water Phantom and Ion Chamber**

**(A) The shielded water tank with Intrabeam source and ion chamber in place. (B) The PTW 34013 soft x-ray ion chamber described below. (C) A cross-section of the 34013. Copyright© – Sethi, Emami, Small and Thomas with CC-BY. [10.3389/fonc.2018.00074](https://doi.org/10.3389/fonc.2018.00074)**

The water tank uses a three-axis stage with position controlled by thumbscrews that correspond to 1 mm per turn. The vertical stage includes an analog readout with a precision of 10  $\mu\text{m}$ . Two separate measuring chamber holders are used for the depth dose and isotropy

measurements (Fig. 9). Each is precisely machined from solid water to fit a PTW Soft X-Ray Ionization Chamber type 34013 (described below). Covers for the measuring chamber holder keep the ion chamber precisely positioned while allowing the cable to pass to the UNIDOS E electrometer through a channel that maintains the shielding of the water tank.



**Figure 9. Spherical Applicator in Water Tank**  
**The water tank with the solid water measuring chamber holders for the isotropy and depth dose measurements visible. The precise window thickness of each holder is printed on top and is approximately 1 mm.**

The depth dose curve is measured in full immersion for each applicator. This matches with the clinical use of the spherical applicator in most cases (i.e. inside brain or breast tissue), but the same cannot be said for the flat and surface applicators. These applicators are intended to work with air lateral to the applicator. As a result, the depth dose *should* be

measured with the water level at the surface of the applicator. Zeiss has acknowledged the difficulty in such a measurement and has indicated that by measuring the flat and surface applicators in full immersion, there is a difference of 1% from measurement with the water level at the surface [17]. Due to the thickness of the measuring chamber holder and the distance from the window to the point of measurement of the ion chamber, the full depth dose curve cannot be measured to a depth of zero. Therefore, Zeiss provides an analytical formula which combines the inverse square law and exponential attenuation. The function roughly fits a depth cubed relationship.

### **2.3.2. Soft X-Ray Chamber**

The PTW 34013 (PTW Freiburg GmbH) parallel plate ionization chamber is used for measuring the depth dose and isotropy. Parallel plate ionization chambers are a type of ionization chamber that are well-suited for measuring depth dose curves. An ionization chamber is a device used for the measurement of ionizing radiation [20]. Using a voltage across two electrodes, the ions created by the radiation are collected by one electrode as a charge which is quantified [20]. The charge collected in the volume is defined as exposure,  $X$ , and has an SI unit of coulombs per kilogram, C/kg [20]. A parallel plate chamber has a geometry in which the two electrodes are circular discs parallel to each other with a very small spacing and thin entrance window of minimal attenuation [20]. The measured exposure can then be converted to absorbed dose, or Gray, which is the amount of energy absorbed per kilogram, J/kg [20]. The conversion is based on intrinsic factors of the detector, the measurement conditions, the spectrum of the radiation, and dose rate [17].

The PTW 34013 chamber has an extremely small volume ( $0.005 \text{ cm}^3$ ) and its point of measurement at the underside of the entrance window make it highly accurate for measuring a depth dose curve in a very steep gradient as is present with the Intrabeam [17]. The PTW

catalog describes the 34013 to be suited for 15-70 keV because of its calibration and flat energy response in this range [21]. The ion chamber is calibrated at an HVL 0.37 mm Al (T30) source. The Intrabeam has a quality of T30 to T50 according to its documentation. The beam quality factor for both T30 and T50 is 1 according to the calibration. Additional details for the specific model 34013 chamber used can be found in section 4.1.

## 2.4. Dosimetric Measurements with OSLDs

### 2.4.1. Landauer nanoDots

This study used nanoDot optically stimulated luminescent dosimeters (Landauer, Inc.) for *in vitro* measurements (Fig. 10). The nanoDot is a 1 cm x 1 cm x 0.2 cm plastic square housing a thin disk (0.3 mm) of aluminum oxide crystal doped with carbon ( $\text{Al}_2\text{O}_3:\text{C}$ ). Because of a variation in sensitivity between nanoDots, each one is tagged with a QR code that contains a serial number and the sensitivity. Their small form factor and measurement accuracy of +/- 5.5% (for screened nanoDots) make them ideal for *in vivo* dosimetry [22].



Figure 10. Landauer nanoDot

### **2.4.2. Optically Stimulated Luminescence**

OSL dosimetry is based on the property of the  $\text{Al}_2\text{O}_3:\text{C}$  crystals which allow them to store energy from ionizing radiation. Upon illumination (at 540 nm), the crystal luminesces (at 420 nm) [2]. The crystal's luminescence is dependent upon both the illumination and the amount of energy stored from radiation [2].

OSLDs use a similar mechanism as thermoluminescent dosimeters (TLD) [2]. The mechanism behind both TLD and OSLD rely on their crystalline structure. The electrons within this structure normally reside in ground energy bands, but with outside energy of sufficient level, like that from radiation, the electrons can move to the conduction band [20]. The dopant (in the case of the OSLDs, carbon) creates traps in the conduction band for these electrons [20]. The electrons remain in the trap until they are stimulated to return to the ground state (by light or heat) [2], [20]. Upon the return to ground state, energy in the form of light is released in what is called luminescence [20]. Because the luminescence is proportional to the number of electrons going to the ground state, and the number of electrons that were excited to the conduction band is proportional to the incident radiation, the luminescence is proportional to the dose of radiation to the crystal [20].

### **2.4.3. Energy Response**

Past studies have noted the over response of OSLDs in the kV range relative to the MV range. Past approximately 600 kV, OSLDs have a flat response making them very useful for dosimetry with modern MV linear accelerators [1], [23], [24]. However, their response in the Intrabeam spectrum is much higher, with response relative to the MV range of 3-4x (Fig. 11) [1], [23]. The difference in response is based on the increased probability of photoelectric interactions in the OSLD than tissue or water [25]. In addition, the response has a steep gradient in this range, so the rapid change in spectrum noted in 2.2.3 impacts the response

as a function of depth with the Intrabeam [23]. This has been studied in the diagnostic energy and dose range with nanoDots irradiated at different depths and different kVp. Differences in the ratio of dose measured with nanoDots to dose measured in an ion chamber were as much as 7% at the 80 kVp range [26].

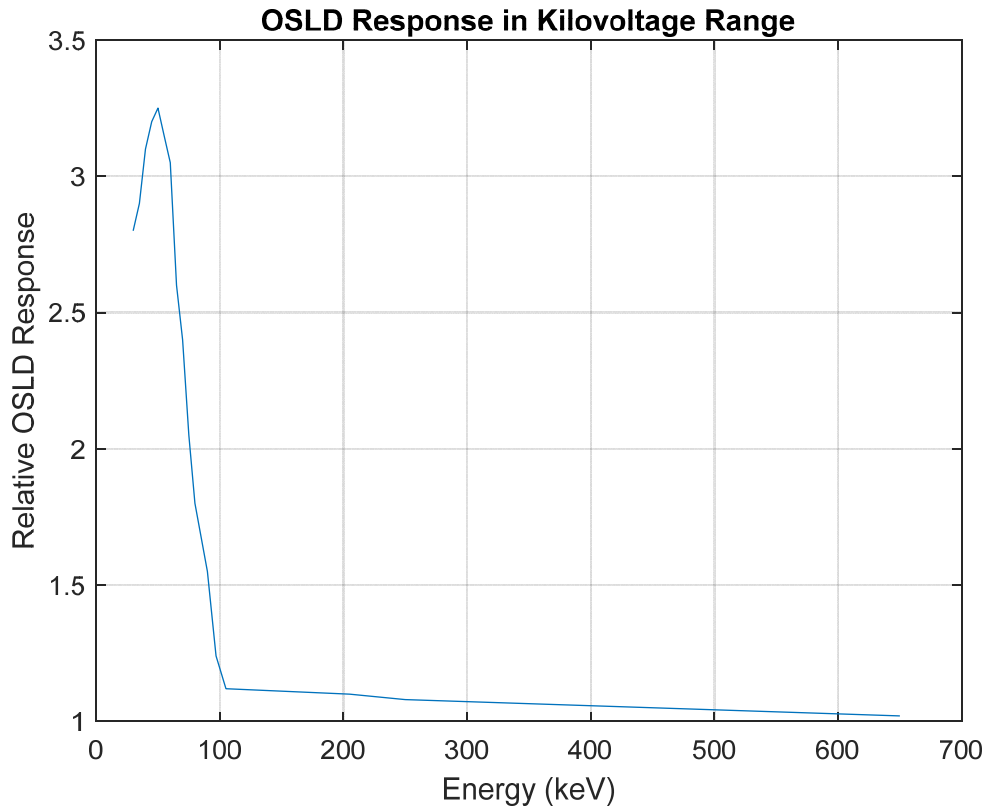


**Figure 11. OSLD Response**  
The relative response of an Al<sub>2</sub>O<sub>3</sub>:C OSLD with respect to energy in the kV range.

#### 2.4.4. microStar Reader and Calibration

The microStar Reader (Landauer, Inc.) is used to read the nanoDots. It utilizes a 532 nm LED light source and band pass filter combination to illuminate the OSL crystal and induce 420 nm luminescence which is incident upon a photomultiplier tube (PMT) [2]. The PMT has two modes for gain based on the dose to the OSLD. The low dose region (<10 cGy) uses a high

gain so that the signal is greater than the background, while for higher doses, lower gain is used so that the PMT is not saturated [1].

Calibrations created with nanoDots are stored in the inLight microStar software and according the *Calibrating the microStar* as follows [1]. The software creates calibration fits based on the sensitivity adjusted counts and known doses received by each individual nanoDot. The fits take a linear form for low doses (<300 cGy) and as non-linear fits in the form of:

$$y = ax^2 + bx + c \quad (1)$$

Where  $y$  is the dose in cGy,  $a$ ,  $b$ , and  $c$  are fit coefficients and  $x$  is the number of counts read by the microStar. The procedure laid out in *Calibrating the microStar* recommends irradiating 3 nanoDots each to a dose of 10, 100, 300, 500, 800, 1000, and 1300 cGy for a non-linear calibration. It also recommends separate calibrations for modalities in the kV range [1].

Landauer offers screened calibration dosimeters (which were used in this study) so that calibration can be performed with the user's desired energy and measurement parameters. In addition, they offer nanoDots that have been pre-exposed to diagnostic dose levels on the surface of a phantom with 80 kVp, 2.9 mm Al HVL x-rays [1]. Because of the varying response in the kV range, conversion factors are also included based on modality use. For example, calibration factors of 1.39 and 1.19 are given for mammography (32 kVp, 0.36 mm Al HVL) and CT (120 kVp, 8.4 mm Al HVL) [1]. However, no such calibration factor exists for the Intrabeam's 0.64 mm Al HVL.

### **3. Methods**

In order to derive a protocol to streamline and allow for reproducible measurements in tissue, several steps were taken. The Intrabeam applicators, prescription doses, and measurement depths were selected. The dose rate at depth was characterized for each applicator in the Intrabeam Water Phantom. To calibrate OSLDs at depth, a 3D printed nanoDot holder was designed to fit in the water phantom's ion chamber holder. The OSLDs were irradiated at discrete depths across all applicators and were read out to determine the number of counts per cGy at depth. Muscle tissue was then harvested from a canine cadaver with thicknesses equivalent to the depths measured in the water phantom. The tissue samples were scanned with computed tomography to determine the tissue attenuation and thickness. The tissues were then irradiated to the prescription dose with OSLDs placed beneath the tissue. The doses were read out on the microStar reader and compared to the original measurements made in the water phantom. The procedure was then analyzed to determine steps in a protocol that would facilitate reliable and reproducible data. A protocol was written with these recommendations.

#### **3.1. Applicator, Prescription, and Depth Selections**

Thus far, the experience with the Intrabeam at OSU has been limited to the spherical applicator, but it is their intent to begin use with the flat and surface applicators. As a result, a dosimetric assessment for all three was desired. The spherical applicators come in diameters from 1.5 to 5.0 cm in 5 mm increments. The 3.5 cm applicator was chosen as it is commonly used clinically and is intermediate in size relative to the others. The flat applicators come in diameters from 1.0 to 6.0 cm in 10 mm increments. The surface applicators come in diameters from 2.0 to 5.0 cm in 10 mm increments. The 3.0 cm applicator was chosen for both the flat and surface applicators because of its intermediate size.

Prescription doses at OSU with the spherical applicator were between 12 and 18 Gy to the surface of the applicator, with 18 Gy being most common. Literature for use of IORT in humans indicate prescription doses on the same order (8-23 Gy) across different cancer types, so 18 Gy was chosen as the base prescription dose for measurements in this research [27]. Depths were selected based on PDD values along with ICRU dose prescription guidelines and values were far below current dose levels available in QUANTEC for organs at risk [28], [29]. For the flat and spherical applicators, depths of 5, 10, and 20 mm were used. Depths of 5 and 20 mm were chosen based on their approximate doses of 50% and 10% at the surface of the applicator. The surface applicator was measured at a depth of 2.8 mm, the minimum depth that could be measured in the water phantom with nanoDots as described below, and 10 mm, with a PDD of approximately 10%. Because the surface applicator's dose is concentrated at the surface, only two depths were measured.

### **3.2. 3D Printed nanoDot Holder**

The Intrabeam Water Phantom uses a precisely machined measuring chamber holder composed of water equivalent plastic. The measuring chamber holder allows for the accurate placement of the ion chamber in the water phantom with a precisely known thickness (printed on the surface of the holder) and air gap (0.5 mm from the holder to the upper housing of the ion chamber) [19].

To facilitate repeatable placement of nanoDots during the calibration procedure, a holder was 3D printed to replicate the shape of the ionization chamber with a space for the nanoDots. The holder was printed using the Ultimaker 2 and designed using Ultimaker Cura out of polylactic acid (PLA). Multiple materials, bead sizes, and infill percentages were tested. A 95% infill and 0.6 mm bead size with PLA were ultimately found to be the optimal combination to create a holder with radiologic properties in the kV range in the range of

water. This was verified by scanning each holder using in a Philips Big Bore Brilliance 16 CT scanner to observe the average Hounsfield Unit of the holder. The combinations of material and printing properties are confirmed to be appropriate in literature [30]–[32]. The final holder can be seen in figure 12. It is composed of two separate pieces that were welded together using a soldering iron. The long piece analogous to the wire of the ion chamber is used as a handle to facilitate removal from the measuring chamber holder. It was also scanned in the CT with a nanoDot in place to determine the distance from the top of the holder to the OSL crystal for use in water tank measurements. This distance, 2.8 mm, was used to apply a shift to ensure equivalent measurement depths between the ion chamber and nanoDots, as described below.

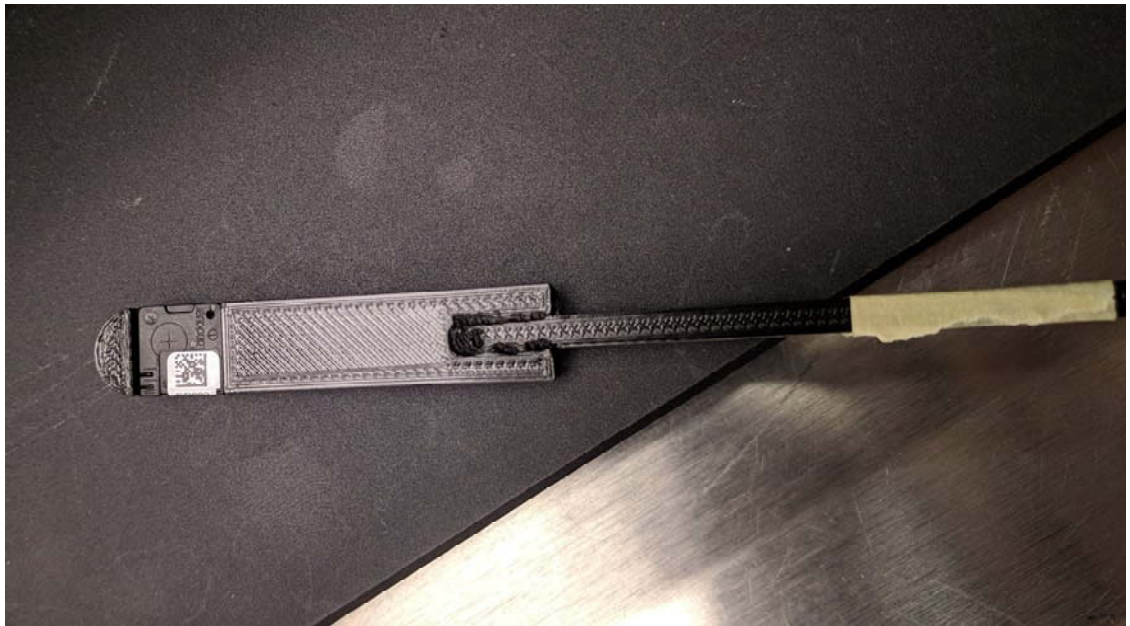


**Figure 12. 3D Printer nanoDot Holder**

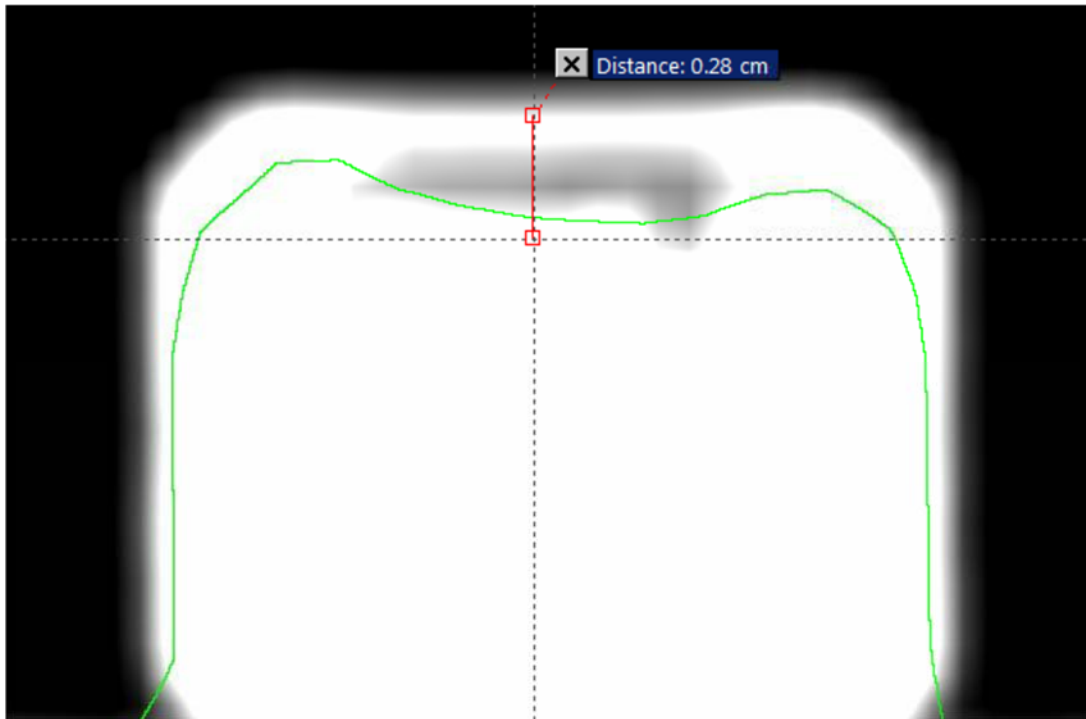


**Figure 13. CT of nanoDot Holder**

**CT scan of the 3D-Printed nanoDot holder in the measuring chamber holder with a nanoDot inside. The distance from the top of measuring chamber holder to the OSL crystal is measured at 0.28 cm.**

### **3.3. Measurement of Dose Rate with Ion Chamber in Water**

Measurements in the Intrabeam Water Phantom with the ion chamber were performed to validate the setup and measurement accuracy against the commissioning data and determine the dose rate at the calibration depths. Routine QA was based on the requirements within the Intrabeam software. This QA procedure includes an output check that gave the pressure and temperature correction factor and showed the deviation of output from calibration (Fig. 14). The instructions for the Intrabeam Water Phantom were then followed to prepare the water tank and center the Intrabeam XRS over the ion chamber [19]. The water phantom is well shielded, but a survey meter was used to check around the room and near the water tank in areas susceptible to leakage for radiation levels, which were shown to be negligible.

|   |          |
|---|----------|
| Dosimeter Reading [pA]                  | 4.953E+1 |
| P&T Correction Factor                   | 9.924E-1 |
| Output Dose Rate [Gy/min]               | 3.403E+0 |
| Deviation from the Calibration File [%] | -4.9     |

**Figure 14. IntraBeam QA with P&T Correction Factor and Output Factor**

After centering the XRS and finding the zero-depth position, the dose rate at zero depth and for each measurement depth was measured for each applicator. It was noted that this zero position was not a true zero. It corresponds to a minimum depth measurable in the water phantom with the ion chamber. Due to the thicknesses of the ion chamber holder (approximately 1 mm), the air gap between the holder and the ion chamber housing (0.5 mm), and the distance from the top of the housing to the measurement point of the ion chamber (0.1 mm), this position was actually at a depth of 1.6 mm. The IntraBeam prescription was entered as 99 Gy to the surface of the applicator, and treatment was paused between each dose rate measurement. This practice optimized the amount of setup time required for each dose rate measurement as setting a prescription before each dose rate measurement would take additional time and require additional QA procedures. The dose rates were compared with the values in the commissioning data. The exact depth positions were noted for positioning of the IntraBeam during OSLD calibrations.

### **3.4. Point Calibration of OSLDs in Water Tank**

To facilitate measurement with nanoDots, the measured gap between the top of the nanoDot holder and the OSL crystal was compared to the gap between the top of the ion chamber and its point of measurement. The difference, 1.2 mm, was used to shift the

measurement depth for each OSLD measurement as shown in figure 15. For each depth and applicator combination, two nanoDots were measured at the prescription dose of 18 Gy to the surface of the applicator in order to prevent inaccuracies from a single bad measurement. There were also spot checks at a prescription dose of 12 Gy performed at the shortest depth for each applicator.

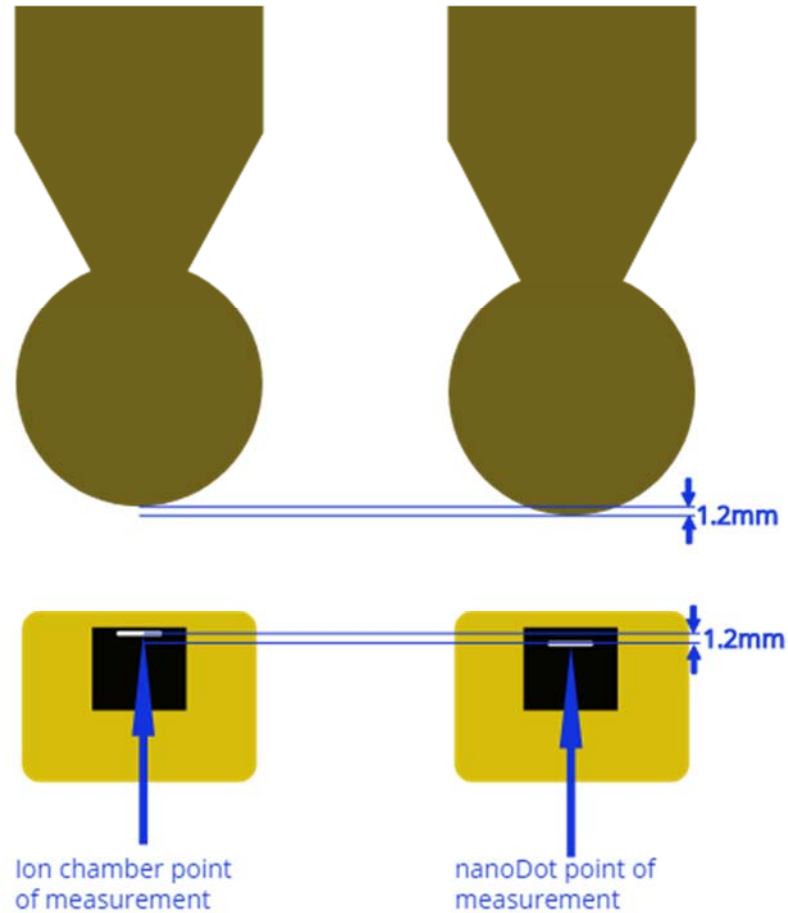


**Figure 15. Shift for difference in measurement point**

For the spherical applicator, prescriptions were entered with the required prescription dose to a treatment depth of 0 mm (the surface of the applicator). However, in the applicator type selection in the Intrabeam software, only the spherical applicator or “None” were available. The prescription for the flat or surface applicators was entered with an applicator type of “None” to a depth of the distance from the XRS to the surface of the applicator (i.e. 18

mm for these applicators). The required prescription had to be modified by dividing the prescription dose by the transfer function ratio determined during commissioning. The transfer function ratio is the ratio of the measured applicator dose rate to the bare XRS dose rate and was 1.92 and 7.21 (unitless ratio) at the surface of the applicators for the flat and surface applicators, respectively. This process is required based on the software version of the Intrabeam that is currently in use at OSU.

When entering the prescription for each applicator, an additional 0.01-0.03 Gy were entered (e.g. 2.49 Gy instead of 2.475 Gy) for the prescription as shown in figure 16. This was done so that the treatment could be stopped a few seconds before completion because after three completed treatments, the Intrabeam requires a QA procedure. While an occasional QA procedure was still required, this practice reduced the number of QAs required.

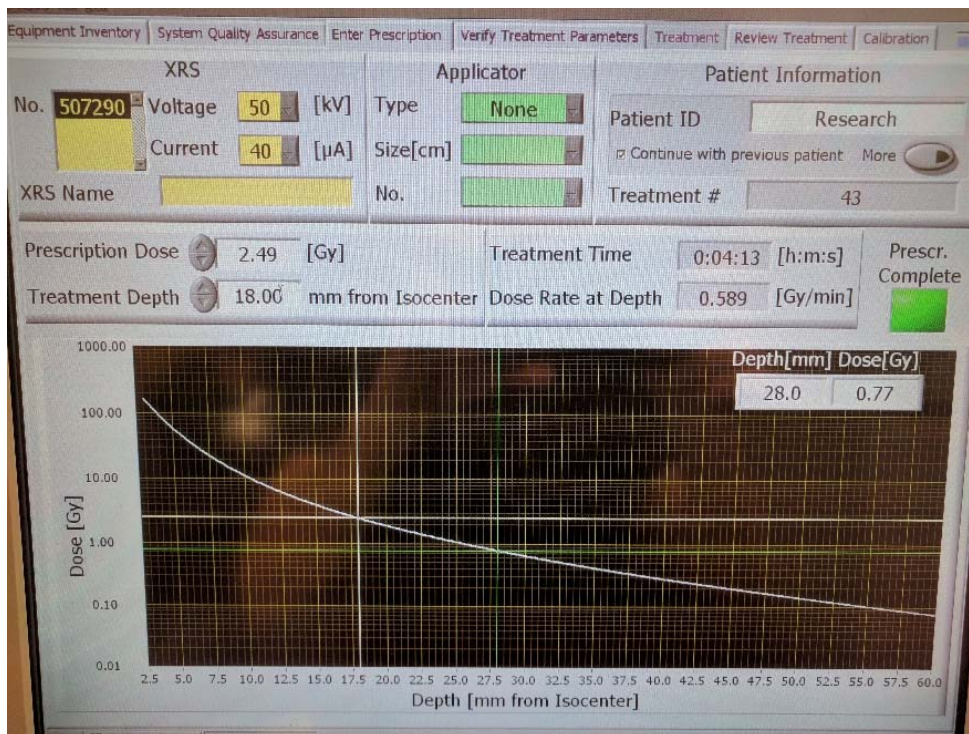


**Figure 16. Entering a Prescription Dose**  
The prescription dose for the surface applicator is entered as 2.49 Gy instead of 2.475 Gy so that the treatment could be stopped early, but the full treatment prescription could be delivered. Note the treatment time is also displayed. This was used to determine the dose delivered to each nanoDot.

The nanoDots were placed as shown in figure 12 with the QR code facing upward and toward the handle of the holder. Because the OSL crystal is slightly off-center of the nanoDot housing, the consistent placement of the nanoDot in the holder was important.

### 3.5. Harvesting Tissue for Measurement

Skeletal muscle samples were collected from a 2.5-year-old greyhound weighing 31 kg that was undergoing diagnostic post-mortem examination at the Oregon Veterinary Diagnostic Laboratory, immediately following euthanasia for reasons unrelated to the study. A new #10 scalpel blade and handle was used to trim in each skeletal muscle tissue sample, taken from the ventral abdominal body wall muscles (i.e. external abdominal oblique, internal abdominal oblique, and transversus abdominis muscles). Four separate skeletal muscle samples of approximately 5 x 5 cm size with 2.8 mm, 5.0 mm, 10.0 mm, and 20.0 mm thickness were prepared. Each sample was individually wrapped in laparotomy sponges moistened with 0.9% NaCl solution, placed in sealed Ziploc bags, and refrigerated at 2° C until use which was within 48 hours of collection.

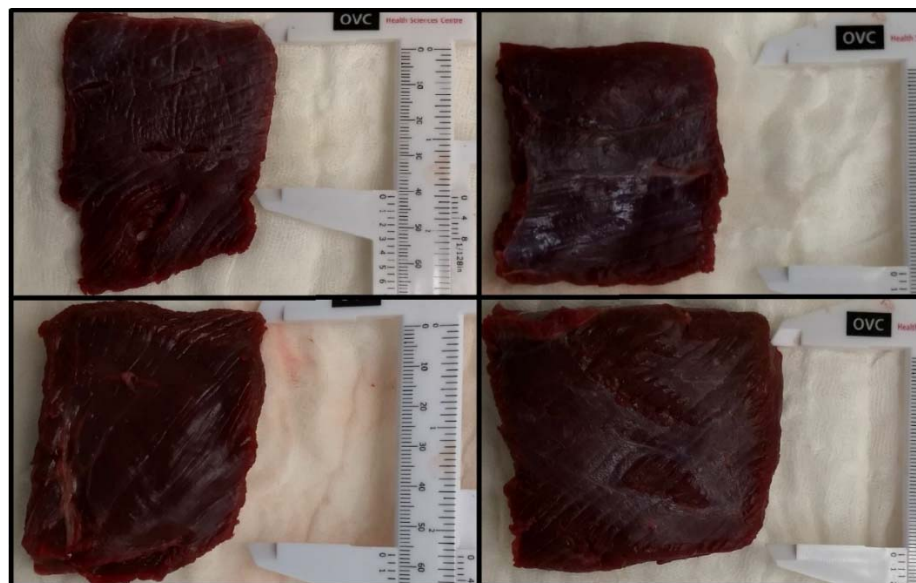
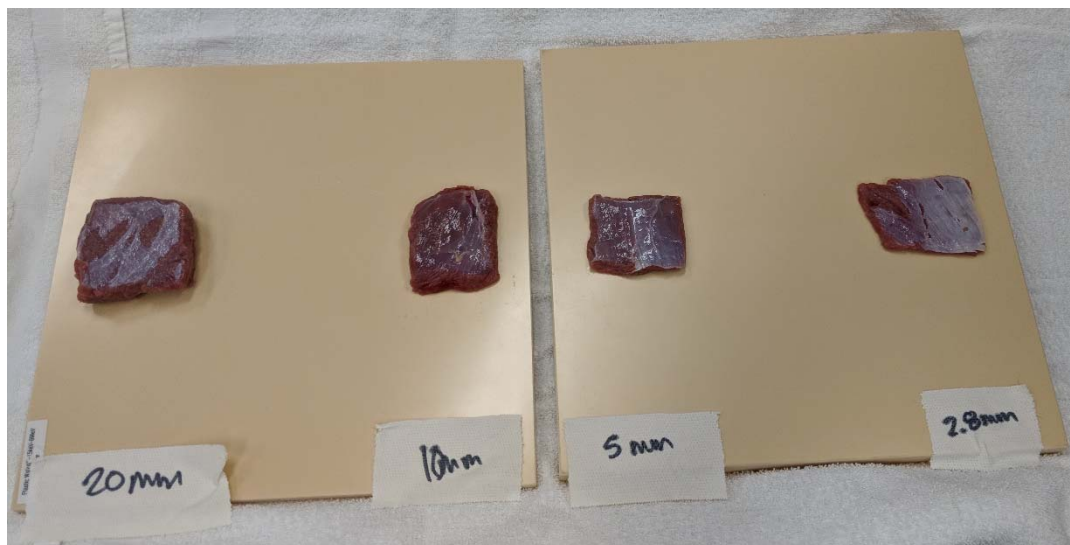


Figure 17. Tissue Samples Immediately After Harvesting

Homogeneous muscle tissue was selected for its similar radiological properties to water. In the range of energies in Intrabeam's spectrum, the mass energy absorption coefficient ratio of muscle to water has a maximum value of approximately 1.04 [33]. Because dose conversion between media is a function of this ratio, the difference between measurements in muscle and water is expected to be within a few percentage points [20], [34]. By establishing a process with consistent measurements to water in muscle tissue, the process could be implemented for other tissue types like adipose, bone, other inhomogeneous media, and full cadavers [35]–[38].

### 3.6. Imaging of Tissue

The tissues were imaged in a Toshiba Aquillion 64 CT scanner to determine their attenuation and thickness. They were placed on Plastic Water® LR – 15 keV – 8 MeV (CIRS, Inc.) in order to provide a flat surface. Each piece of tissue was placed with the epimysium facing up for consistency (Fig. 18). The images were analyzed in K-PACS (IMAGE Information Systems Ltd.) at a window and level value of 400 and 0, respectively.



**Figure 18. Tissue on Plastic Water before CT**  
The tissue samples labeled with thickness on the CT couch. They are placed on Plastic Water to ensure they lay flat. The epimysium is facing up.

### 3.7. Irradiation of Tissue

A strip of bolus was placed in the cavity of a slab of Plastic Water to provide a surface for the nanoDot that would prevent any slipping during tissue placement as seen in figure 19. The Plastic Water had a grid pattern that simplified centering the tissue and Intrabeam applicator over the nanoDot. Care was taken to ensure that the applicators were placed perpendicular to the sample and that the applicator was in contact with the tissue without providing an amount of pressure that would significantly change the thickness of the tissue (Fig. 20).

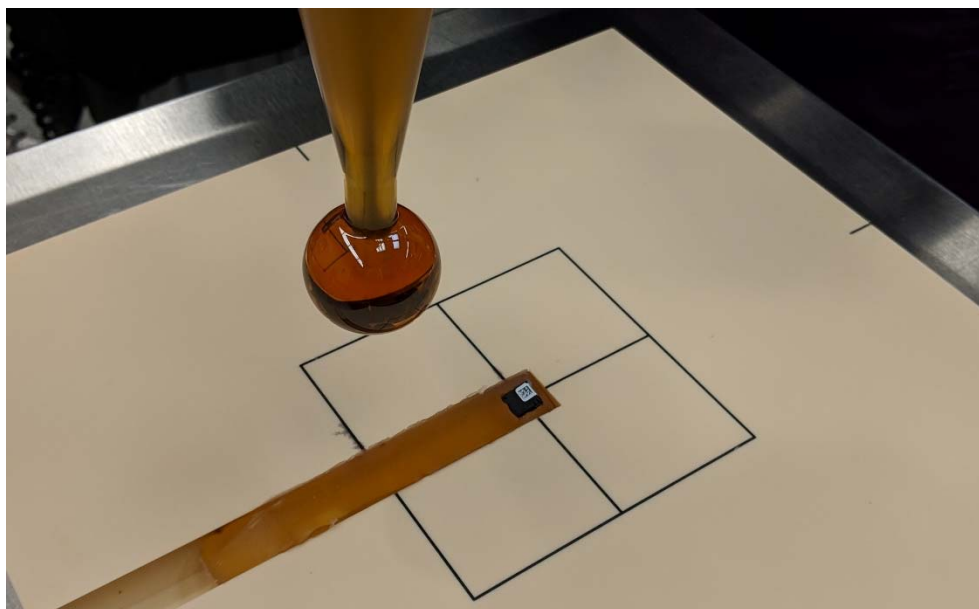


**Figure 19. nanoDot Placed for Measurement**

**A nanoDot is placed on a thin strip of bolus in the ion chamber channel of the Plastic Water. The bolus created a tacky surface that prevented the nanoDot from slipping during tissue placement. The grid also provided a reference for placement and centering of the tissue and Intrabeam applicator.**

Each applicator and tissue thickness combination were based on the combinations measured in section 3.4. For each, two nanoDots were irradiated to an applicator prescription of 18 Gy. The tissue was only removed from its storage cooler and wrapping immediately before irradiating. After irradiation it was placed back in the cooler as the samples heated significantly during treatment.

Mobile glass shielding and lead vests were used for shielding [39]. A mobile shield was placed between the Intrabeam and the door. Lead vests were hung closer to the Intrabeam. A survey meter was used to monitor exposure in the room. As there was still some radiation at the control console, the researchers left the room during treatment. An additional mobile shield and signage was placed at the entrance, and entry to the room was monitored.

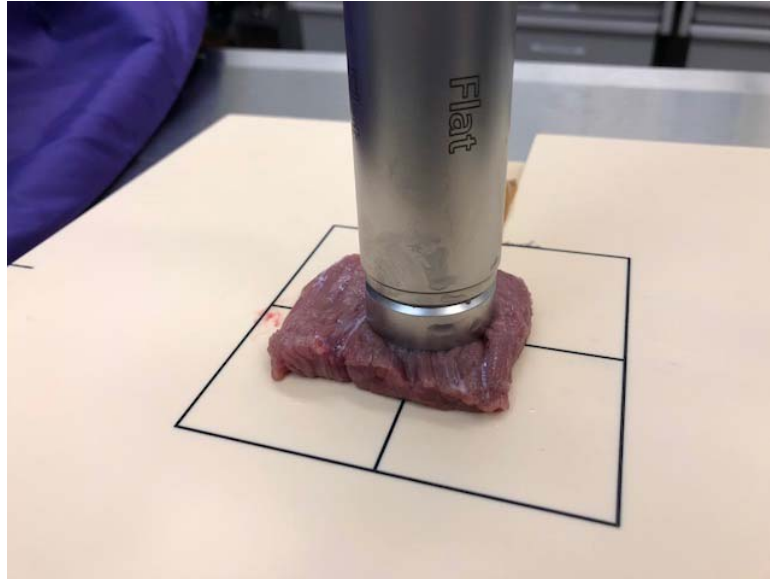


**Figure 20. Flat Applicator on Tissue**

**The flat applicator placed over a tissue sample. Care was taken to ensure that the applicator was perpendicular to the tissue with contact to the entire surface of the applicator while not applying excessive pressure on the tissue.**

## 4. Results

### 4.1. Ion Chamber Measurements

The ion chamber was connected to a UNIDOS E electrometer which gave an output of in nC for the charge collected by the ion chamber over the course of one minute. The dose rate was then found using the following equation defined by the instruction manual [19]:

$$D_w(r) \left[ \frac{Gy}{min} \right] = N_k \left[ \frac{Gy}{C} \right] \times Q(r)[C] \times \frac{T[K]}{T_0[K]} \times \frac{P_0[hPa]}{P[hPa]} \times k_Q \times k_{Ak \rightarrow Dw} \times 1 \left[ \frac{1}{min} \right] \quad (2)$$

Where:

$\dot{D}_w(r)$  is the dose rate to water at depth  $r$ .

$N_k$  is the detector calibration factor that is given with the ion chamber's calibration certificate.

$Q(r)$  is the measured charge at depth  $r$ .

$T$  and  $T_0$  refer to the temperature and reference temperature at calibration.

$P$  and  $P_0$  refer to the pressure and reference pressure at calibration.

$k_Q$  is the beam quality correction factor given with the calibration certificate.

$k_{Ak \rightarrow Dw}$  is the correction factor for the ion chamber from air kerma to dose to water provided by the manufacturer.

The detector calibration factor was given as  $5.69\text{E}+09 \text{ Gy/C}$ , the beam quality correction factor for the Intrabeam was 1 (although some research indicates a slight variation in quality factor among different applicators, it varies less than 1% [40]), and the ion chamber correction factor from air kerma to dose to water was 1.054. The temperature and pressure are included in a single T&P correction factor that varied between measurement days. It was reported by the Intrabeam QA to be 0.9924 during the first day and 1.008 during the second. Using these factors and equation 1, the results of the ion chamber measurements can be seen in table 1.

**Table 1. Ion Chamber Results**

| <b>Applicator</b> | <b>Depth (mm)</b> | <b>PDD</b> | <b>Dose Rate Measured (Gy/min)</b> | <b>Dose Rate at Commissioning (Gy/min)</b> | <b>Percent Difference</b> |
|-------------------|-------------------|------------|------------------------------------|--|---------------------------|
| Surface 3-cm      | 2.8               | 39.8%      | 1.7                                | 1.755                                      | -3.13%                    |
| Surface 3-cm      | 10                | 9.3%       | 0.399                              | 0.412                                      | -3.16%                    |
| Sphere 3.5-cm     | 5                 | 55.1%      | 0.589                              | **   | **                        |
| Sphere 3.5-cm     | 10                | 29.5%      | 0.315                              | **   | **                        |
| Sphere 3.5-cm     | 20                | 10.6%      | 0.113                              | **   | **                        |
| Flat 3-cm         | 5                 | 43.3%      | 0.506                              | 0.482                                      | 4.98%                     |
| Flat 3-cm         | 10                | 21.3%      | 0.248                              | 0.2479                                     | 0.04%                     |
| Flat 3-cm         | 20                | 7.8%       | 0.091                              | 0.0898                                     | 1.34%                     |

\*\* While the spherical commissioning data was available for comparison at the treatment console, it was not recorded and it was not available offsite like the surface and flat applicators. It will be included as a later addendum.

## **4.2. nanoDot Measurements in the Intrabeam Water Phantom**

The dose delivered to the nanoDots was calculated by multiplying the dose rate at each depth measured in 3.3 by the treatment time determined by the Intrabeam for each prescription dose and applicator type. The nanoDots were measured in the microStar reader with each OSLD being read 3 times [1]. Each measurement was carried out within 3 days but no less than 24 hours after irradiation. This eliminated the possibility of an influence from superficial traps noted in the literature [2], [3], [23]. The microStar reader gave raw counts from each OSLD because a full calibration had not been performed. The counts were corrected with the sensitivity of each nanoDots, as indicated by the microStar reader. The counts per cGy were then calculated based on the dose delivered to each nanoDot. The results are in Table 2. The delivered dose in column 3 is based on the product of the dose rate measured in the water tank multiplied by the total treatment time for each measurement. There were no obvious trends in the counts/cGy with depth. Variations for measurements at the same depth were present. The results are displayed in a scatter plot in figure 21.

**Table 2. Preliminary nanoDot Water Tank Results**

| Applicator    | Depth (mm) | Delivered Dose (Gy) | Nanodot Count | Counts/cGy |
|---------------|------------|---------------------|---------------|------------|
| Surface 3-cm  | 2.8        | 7.17                | 2010794       | 2804.5     |
| Surface 3-cm  | 2.8        | 4.78                | 1350536       | 2825.4     |
| Surface 3-cm  | 10         | 1.68                | 463469.4      | 2758.7     |
| Sphere 3.5-cm | 5          | 9.92                | 2732815       | 2754.9     |
| Sphere 3.5-cm | 5          | 6.61                | 1946960       | 2945.5     |
| Sphere 3.5-cm | 10         | 5.31                | 1527185       | 2876.1     |
| Sphere 3.5-cm | 20         | 1.9                 | 568575        | 2992.5     |
| Flat 3-cm     | 5          | 7.79                | 2165745       | 2780.2     |
| Flat 3-cm     | 5          | 5.21                | 1478706       | 2838.2     |
| Flat 3-cm     | 10         | 3.83                | 1094267       | 2857.1     |
| Flat 3-cm     | 20         | 1.4                 | 367718.3      | 2626.6     |

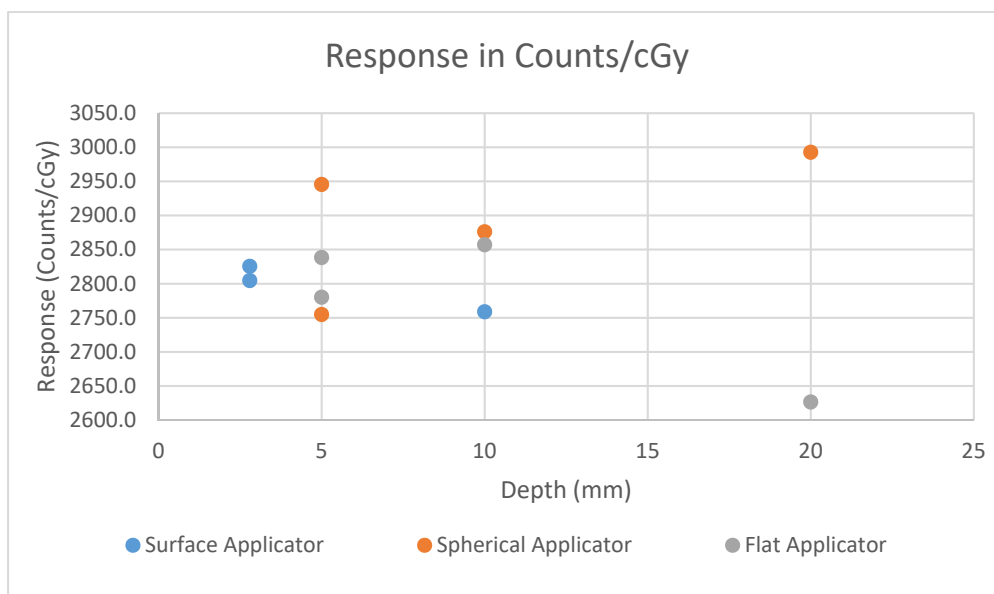


**Figure 21. Response in Counts per cGy by Applicator**  
**Response in counts per cGy for each applicator based on depth in mm. There is no observable consistent trend in a change in response with depth between applicators. The response increases in the spherical applicator as the beam hardens, but it decreases for the surface and flat applicators.**

## 4.3. Harvested Tissue

### 4.3.1. CT Measurements

Measurement of the tissue with the CT took place after irradiation. For the 2.8, 5, and 20 mm samples, nanoDots were placed under the center of the tissue sample. However, for the 10 mm sample, the thickness at the center was noticeably large, so irradiation took place approximately halfway between the center and the edge of the sample. The measurements made in K-PACS can be seen in figure 22. For the intended thicknesses of 2.8, 5, 10, and 20 mm, it was found that the actual thicknesses were 5.9, 8.3, 12.6, and 24.2 mm, respectively. The mean Hounsfield Units of each sample were 59, 68, 74, and 83, respectively.

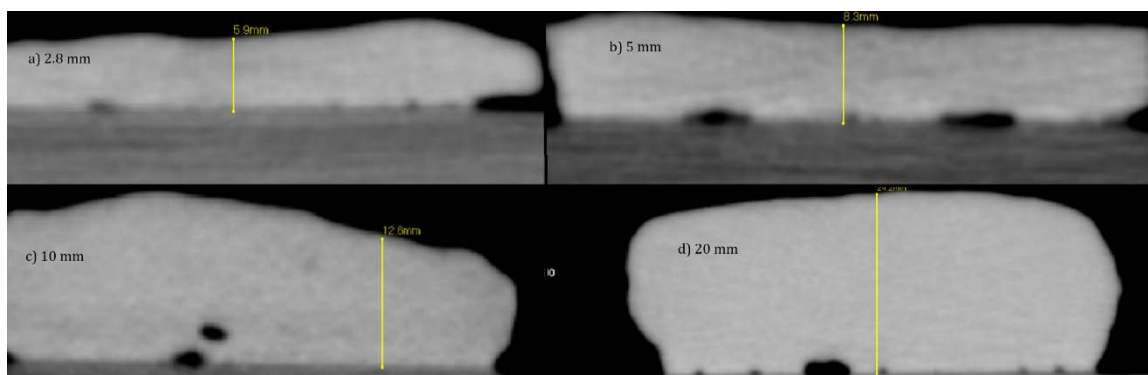


**Figure 22. Tissue CTs**

**The CT scans of the tissue samples. The measurements show that the deviation from the intended dimension was significant. The samples, labeled a-d) were intended to be 2.8, 5, 10, and 20 mm, respectively. The measurements show that the actual thicknesses were 5.9, 8.3, 12.6, and 24.2 mm.**

## 4.4. *in vitro* Measurements

The results for the measurements in tissue are found in table 3. Because the tissue thicknesses deviated greatly from the measurements made at depth in water, comparison is difficult as can be seen by the percentage differences in table 4.

**Table 3. Preliminary Counts at Depth in Tissue**

| <b>Applicator</b> | <b>CT Depth (mm)</b> | <b>Count @ CT Depth in Tissue</b> |
|-------------------|----------------------|-----------------------------------|
| Surface 3-cm      | 5.9                  | 852983.6                          |
| Surface 3-cm      | 12.5                 | 326091.8                          |
| Sphere 3.5-cm     | 8                    | 1603376.0                         |
| Sphere 3.5-cm     | 12.5                 | 1256020.0                         |
| Sphere 3.5-cm     | 24                   | 461449.6                          |
| Flat 3-cm         | 8                    | 1293620.0                         |
| Flat 3-cm         | 12.5                 | 665129.6                          |
| Flat 3-cm         | 24                   | 319698.5                          |

**Table 4. Preliminary Counts in Tissue Relative to Water**

| <b>Applicator</b> | <b>Desired Depth (mm)</b> | <b>CT Depth (mm)</b> | <b>Count @ Desired Depth in Water</b> | <b>Count @ CT Depth in Tissue</b> | <b>Percent Difference</b> |
|-------------------|---------------------------|----------------------|---------------------------------------|-----------------------------------|---------------------------|
| Surface 3-cm      | 2.8                       | 5.9                  | 2010794.0                             | 852983.6                          | -57.6%                    |
| Surface 3-cm      | 10                        | 12.5                 | 463469.4                              | 326091.8                          | -29.6%                    |
| Sphere 3.5-cm     | 5                         | 8                    | 2732815.0                             | 1603376.0                         | -41.3%                    |
| Sphere 3.5-cm     | 10                        | 12.5                 | 1527185.0                             | 1256020.0                         | -17.8%                    |
| Sphere 3.5-cm     | 20                        | 24                   | 568575.0                              | 461449.6                          | -18.8%                    |
| Flat 3-cm         | 5                         | 8                    | 2165745.0                             | 1293620.0                         | -40.3%                    |
| Flat 3-cm         | 10                        | 12.5                 | 1094267.0                             | 665129.6                          | -39.2%                    |
| Flat 3-cm         | 20                        | 24                   | 367718.3                              | 319698.5                          | -13.1%                    |

#### **4.5. Protocol**

As this study had a primary goal of deriving a protocol that could facilitate a dosimetric assessment of the Intrabeam in a canine tissue model using OSLDs, a protocol was generated. This protocol is detailed in Appendix A. Assumptions are provided based on the equipment available and clinical needs. The protocol refers the researcher to resources that provide certain steps, like setting up the water tank or creating a nanoDot calibration. It also provides

more detailed strategies for items that are very specific to this study, like depth selection and tissue harvesting.

## **5. Discussion**

### **5.1. Ion Chamber Measurements**

Measurements were made with the ion chamber in the water tank to establish the dose rate for each applicator at each discrete depth. Spot checks at other depths were also performed. Each of these measurements compared favorably to commissioning data with deviation in dose rate that did not exceed 5%. This deviation is acceptable as the dose rate is known to vary as can be seen in Figure 14 where a 4.9% deviation was found during QA. The PAICH used during QA checks the dose output, compares it to commissioning data, and sets the treatment time based on the dose rate. The resulting dose rates measured in table 1 were used to calculate the dose received by each nanoDot for the nanoDot measurements in the Intrabeam Water Phantom.

### **5.2. nanoDot Measurements in the Intrabeam Water Phantom**

The values of each nanoDot for each depth and dose level were consistent with each other. The coefficient of variation (standard deviation/mean) for each was less than 1%, which is good according to the manual [1]. However, there was no meaningful trend notable in the change in response (in counts/cGy) with depth. An increased response can be seen in the spherical applicator with depth. This was expected based on the hardening of the beam and the increased intrinsic response of OSLDs as the mean beam energy approached 50 kV [2], [4], [23]. This finding was not repeated with the flat or surface applicators. The flat applicator's response seemed to decrease slightly with depth, while the change in response with the surface applicator showed a decrease with depth, but the magnitude of this change was minimal.

In addition, for irradiations to different dose prescriptions at the same depth, there was a difference in response of between 1 and 7%. Studies have shown a change in response with accumulated dose with a peak in response around 600 cGy [3]. However, these studies were done with the dose level being modulated based on depth rather than performing all measurements at the same depth.

These findings do not provide a meaningful or significant result. With both inconsistent results with dose accumulation and depth, more complete calibrations are necessary. A calibration with additional dose levels and multiple nanoDots per dose level at each depth are necessary for a full treatment of this problem.

### **5.3. Harvested Tissue**

The large variability from desired proved to be the largest obstacle to consistent measurements. It is clear that the procedure used for harvesting tissue was not adequate for producing tissues of very accurate thicknesses. Even a small variation in thickness can be problematic for the thinnest of samples. For example, considering the 2.8 mm thickness and the surface applicator, a +/- 0.5 mm error would cause an error in dose of approximately 15%. By increasing this thickness to 5 mm where the dose gradient is not as steep, a 0.5 mm error would decrease the error in dose to 10%. A possible solution is recommended in the protocol in Appendix A. It, along with other procedures, will be investigated further.

The muscle HU values were slightly higher than generally accepted values for muscle which are typically stated as around 40 HU [41]. However, the values are fairly close and may indicate that these muscles are denser than typical human muscle. It should also be noted that the CT scanner is not ACR accredited, so its HU accuracy is not guaranteed. This should also be considered when using the measured thicknesses on the CT scanner. It is

recommended that a phantom, like the CatPhan®, be used to validate the measurement accuracy of the scanner before tissues are measured.

#### **5.4. *in vitro* Measurements**

As explained above, muscle tissue measurements were made because they were expected to be similar to those made in water. The variation in mass energy absorption coefficient ratio indicated that the dose should increase by a factor of 2-4% [33]. However, this was not seen due to the very different measurement conditions between the water tank and tissue measurements. Both of these indicate the importance of identical measurement conditions with variables limited as much as possible so that the change in media from water to muscle is the largest factor in measurement difference.

The experimental setup for the spherical tissue measurement differed from clinical use in humans, which involve the spherical applicator being entirely enveloped in tissue. As a result, there is a loss of scatter from the tissue on the sides of the applicator. However, in clinical use at OSU, this is not the case as many treatments with the spherical applicator are directly against areas in the mouth which do not envelope the applicator. Thus, the experimental setup is an accurate representation for clinical use. Zeiss's experiments indicate that there is very little difference in the performance of the calibrations of the flat and surface applicators in full immersion and with the water at the surface, but an investigation of the immersion of the spherical applicator may also be warranted [19].

#### **5.5. Sources of Variability and Recommended Protocol**

Several sources of variability have been identified in this study. These are listed in table 6 with potential solutions. These solutions are included as part of the protocol, Appendix A, that is the main outcome of this study. The largest impact on this study was the variation in

thickness from the desired values for the muscle tissue. This variation led to differences in expected depth dose up to 52%. Other issues that made analysis impossible were the lack of complete nanoDot calibrations and few data points. As full calibrations were not completed, the cause for inconsistencies in response at a single depth and at various depths were impossible to determine. With these sources of variability in mind, an error propagation study should be performed to determine the total uncertainty. This should include uncertainties in setup and the calibration data.

**Table 5. Sources of Variability and Potential Solutions**

| <b>Source of Variability/Uncertainty</b> | <b>Potential Solution</b>   |
|--|---|
| Tissue thickness                         | Use of commercial meat slicer for uniform thicknesses. Limiting to a single reproducible thickness that is stackable. |
| Single point calibration per depth       | Create a full calibration   |
| Few data points                          | At least two nanoDots irradiated for each applicator, prescription dose, and thickness/depth measured.                |

## 6. Future Directions

This study has several future goals in order to perform a complete dosimetric assessment of the Intrabeam in veterinary medicine. A completion of nanoDot calibrations across several depths is necessary to determine the impact of the OSLD response with depth. The use of pre-irradiated diagnostic nanoDots may also be useful in making baseline low dose measurements. A full calibration to the doses expected in a treatment are still necessary, but these preirradiated dosimeters may be used to validate experimental setup.

While the impact of full immersion is minimal for water tank measurements with the surface and flat applicators is minimal per the manual for the water phantom, the same cannot be assumed for the spherical applicator [17]. Because the spherical applicator does not have lead attenuation to its sides, the effect of scatter from the area may have an effect.

An investigation on the affect to dose at depth both in full immersion and with the spherical applicator placed in contact with the water's surface as performed with tissue should be completed. Based on the measured effect, a modification of the protocol may be necessary.

With a repeatable procedure for the harvesting of consistent animal tissue, an assessment in muscle should be completed. It is then suggested that an assessment in other homogeneous tissues be performed. Adipose tissue is a possible candidate, although it is acknowledged that there is difficulty in obtaining full thickness homogeneous samples of all tissue types. A rigorous investigation of the impact of bone should be completed as commonly performed treatments, like those in the mouth, can rely on the shielding provided by the hard palate to decrease dose to critical structures in the cranium. Finally, the study can expand to an investigation in an in-tact cadaver with treatments of many tissue types performed.

## **7. Conclusion**

A study was performed to make initial measurements and derive a protocol that lays out the steps necessary for an *in vitro* dosimetric assessment of the Intrabeam with OSLDs. Initial measurement results were not statistically significant because of systematic errors. The study identified procedures that led to these errors and made recommendations to avoid them in the future. A protocol was written with templates for data collection.

## 8. References

- [1] Clifford J. Yahnke, "Calibrating the microStar." Landauer, June-2009.
- [2] P. A. Jursinic, "Characterization of optically stimulated luminescent dosimeters, OSLDs, for clinical dosimetric measurements," *Med. Phys.*, vol. 34, no. 12, pp. 4594–4604, Dec. 2007.
- [3] T. Bryant, "Saturation And Response Dependence Of Oslds And Microstar Reader In The High Dose Range For Intrabeam Kv X-rays And Initial Investigation Into The Use Of Gafchromic Film As An In Vivo Dosimeter In The High Dose Region," *Sch. Arch.*, Sep. 2017.
- [4] M. A. Ebert, A. H. Asad, and S. A. Siddiqui, "Suitability of radiochromic films for dosimetry of low energy X-rays," *J. Appl. Clin. Med. Phys.*, vol. 10, no. 4, pp. 232–240, Sep. 2009.
- [5] D. Gardner, "Spontaneous squamous cell carcinomas of the oral region in domestic animals: a review and consideration of their relevance to human research," *Oral Dis.*, vol. 2, no. 2, pp. 148–154, Jun. 2008.
- [6] B. Hernandez, H. Adissu, B.-R. Wei, H. Michael, G. Merlino, and R. Simpson, "Naturally Occurring Canine Melanoma as a Predictive Comparative Oncology Model for Human Mucosal and Other Triple Wild-Type Melanomas," *Int. J. Mol. Sci.*, vol. 19, no. 2, p. 394, Jan. 2018.
- [7] B. M. Matz, "Current Concepts in Oncologic Surgery in Small Animals," *Vet. Clin. North Am. Small Anim. Pract.*, vol. 45, no. 3, pp. 437–449, May 2015.
- [8] B. Séguin, "Canine Soft Tissue Sarcomas: Can Being a Dog's Best Friend Help a Child?," *Front. Oncol.*, vol. 7, Nov. 2017.
- [9] M. Milovancev and D. S. Russell, "Surgical margins in the veterinary cancer patient: Surgical margins in the veterinary cancer patient," *Vet. Comp. Oncol.*, vol. 15, no. 4, pp. 1136–1157, Dec. 2017.
- [10] S. M. LaRue and J. T. Custis, "Advances in Veterinary Radiation Therapy," *Vet. Clin. North Am. Small Anim. Pract.*, vol. 44, no. 5, pp. 909–923, Sep. 2014.
- [11] H. Gardner, J. Fidel, G. Haldorson, W. Dernell, and B. Wheeler, "Canine oral fibrosarcomas: a retrospective analysis of 65 cases (1998-2010)," *Vet. Comp. Oncol.*, vol. 13, no. 1, pp. 40–47, Mar. 2015.
- [12] J. S. Vaidya *et al.*, "Targeted intraoperative radiotherapy versus whole breast radiotherapy for breast cancer (TARGIT-A trial): an international, prospective,

- randomised, non-inferiority phase 3 trial," *The Lancet*, vol. 376, no. 9735, pp. 91–102, Jul. 2010.
- [13] "INTRABEAM System - Medical Technology | ZEISS United States." [Online]. Available: <https://www.zeiss.com/meditec/us/products/intraoperative-radiotherapy/intrabeam-system.html>. [Accessed: 24-May-2018].
- [14] Q. Liu, F. Schneider, L. Ma, F. Wenz, and C. Herskind, "Relative Biologic Effectiveness (RBE) of 50 kV X-rays Measured in a Phantom for Intraoperative Tumor-Bed Irradiation," *Int. J. Radiat. Oncol. • Biol. • Phys.*, vol. 85, no. 4, pp. 1127–1133, Mar. 2013.
- [15] D. J. Eaton, "Quality assurance and independent dosimetry for an intraoperative x-ray device," *Med. Phys.*, vol. 39, no. 11, pp. 6908–6920, Nov. 2012.
- [16] J. Beatty *et al.*, "A new miniature x-ray device for interstitial radiosurgery: Dosimetry," *Med. Phys.*, vol. 23, no. 1, pp. 53–62, Jun. 1998.
- [17] Carl Zeiss Meditec, "INTRABEAM Water Phantom Instructions for Use." 2012.
- [18] F. Schneider, S. Clausen, J. Thölking, F. Wenz, and Y. Abo-Madyan, "A novel approach for superficial intraoperative radiotherapy (IORT) using a 50 kV X-ray source: a technical and case report," *J. Appl. Clin. Med. Phys.*, vol. 15, no. 1, pp. 167–176, Jan. 2014.
- [19] L. A. Kelley, R. W. Holt, and T. W. Rusch, "Spectral Comparison of the Xovert and Zeiss 50 kVp X-ray Systems," p. 14.
- [20] F. M. Khan and J. P. Gibbons, *Khan's the physics of radiation therapy*, Fifth edition. Philadelphia, PA: Lippincott Williams & Wilkins/Wolters Kluwer, 2014.
- [21] "PTW: Soft X-Ray Ionization Chambers." [Online]. Available: [http://www.ptw.de/soft\\_x-ray\\_chambers0.html](http://www.ptw.de/soft_x-ray_chambers0.html). [Accessed: 26-May-2018].
- [22] "nanoDot™ - Dosimetry Badges | LANDAUER." [Online]. Available: <https://www.landauer.com/product/nanodot>. [Accessed: 26-May-2018].
- [23] S. Fry, "The clinical use of OSLD," presented at the Spring Clinical AAPM Meeting 2015.
- [24] Y. Poirier, S. Kuznetsova, and J. E. Villarreal-Barajas, "Characterization of nanoDot optically stimulated luminescence detectors and high-sensitivity MCP-N thermoluminescent detectors in the 40–300 kVp energy range," *Med. Phys.*, p. n/a-n/a.
- [25] S. B. Scarboro and S. F. Kry, "Characterisation of energy response of Al<sub>2</sub>O<sub>3</sub>:C optically stimulated luminescent dosimeters (OSLDs) using cavity theory," *Radiat. Prot. Dosimetry*, vol. 153, no. 1, pp. 23–31, Jan. 2013.

- [26] L. Lavoie, M. Ghita, L. Brateman, and M. Arreola, "Characterization of a Commercially-Available, Optically-Stimulated Luminescent Dosimetry System for Use in Computed Tomography," *Health Phys.*, vol. 101, no. 3, p. 299, Sep. 2011.
- [27] B. J. Debenham, K. S. Hu, and L. B. Harrison, "Present status and future directions of intraoperative radiotherapy," *Lancet Oncol.*, vol. 14, no. 11, pp. e457–e464, Oct. 2013.
- [28] C. Mayo, M. K. Martel, L. B. Marks, J. Flickinger, J. Nam, and J. Kirkpatrick, "Radiation Dose–Volume Effects of Optic Nerves and Chiasm," *Int. J. Radiat. Oncol. • Biol. • Phys.*, vol. 76, no. 3, pp. S28–S35, Mar. 2010.
- [29] International Commission on Radiation Units and Measurements, Ed., *Prescribing, recording, and reporting photon beam therapy*. Bethesda, Md: International Commission on Radiation Units and Measurements, 1999.
- [30] S. Burlison, J. Baker, A. T. Hsia, and Z. Xu, "Use of 3D printers to create a patient-specific 3D bolus for external beam therapy," *J. Appl. Clin. Med. Phys.*, vol. 16, no. 3, pp. 166–178, May 2015.
- [31] O. L. Dancewicz, S. R. Sylvander, T. S. Markwell, S. B. Crowe, and J. V. Trapp, "Radiological properties of 3D printed materials in kilovoltage and megavoltage photon beams," *Phys. Med.*, vol. 38, pp. 111–118, Jun. 2017.
- [32] T. Kairn, S. B. Crowe, and T. Markwell, "Use of 3D Printed Materials as Tissue-Equivalent Phantoms," in *World Congress on Medical Physics and Biomedical Engineering, June 7-12, 2015, Toronto, Canada*, Springer, Cham, 2015, pp. 728–731.
- [33] H. E. Johns and J. R. Cunningham, *Physics of Radiology, Fourth Edition*, 4 edition. Springfield, Ill., U.S.A: Charles C Thomas Pub Ltd, 1983.
- [34] E. B. Podgoršak, *Radiation physics for medical physicists*, 2nd, enl. ed ed. Heidelberg: Springer, 2010.
- [35] P. J. Lanzon and G. C. Sorell, "The effect of lead underlying water on the backscatter of X-rays of beam qualities 0.5 mm to 8 mm Al HVT," *Phys. Med. Biol.*, vol. 38, no. 8, p. 1137, 1993.
- [36] A. Sethi, B. Chinsky, S. Gros, A. Diak, B. Emami, and W. Small Jr, "Tissue inhomogeneity corrections in low-kV intra-operative radiotherapy (IORT)," *Transl. Cancer Res.*, vol. 4, no. 2, pp. 182–188, Apr. 2015.
- [37] J. Baines, S. Zawlodzka, T. Markwell, and M. Chan, "Measured and Monte Carlo simulated surface dose reduction for superficial X-rays incident on tissue with underlying air or bone," *Med. Phys.*, p. n/a-n/a.

- [38] B. J. Healy, S. Sylvander, and K. N. Nitschke, "Dose reduction from loss of backscatter in superficial x-ray radiation therapy with the Pantak SXT 150 unit," *Australas. Phys. Eng. Sci. Med.*, vol. 31, no. 1, pp. 49–55, Mar. 2008.
- [39] D. J. Eaton, R. Gonzalez, S. Duck, and M. Keshtgar, "Radiation protection for an intra-operative X-ray device," *Br. J. Radiol.*, vol. 84, no. 1007, pp. 1034–1039, Nov. 2011.
- [40] M. Goubert and L. Parent, "Dosimetric characterization of INTRABEAM® miniature accelerator flat and surface applicators for dermatologic applications," *Phys. Med.*, vol. 31, no. 3, pp. 224–232, May 2015.
- [41] J. T. Bushberg, J. A. Seibert, E. M. L. Jr, and J. M. Boone, *The Essential Physics of Medical Imaging, Third Edition*, Third, North American edition. Philadelphia: LWW, 2011.

## 9. Appendix

### A. Suggested Protocol for Intrabeam OSL Dosimetric Assessment

**The following assumptions are made for the implementation of this protocol:**

- A. The applicator, prescriptions, and tissue types are predetermined.
  - 1. The applicator has been commissioned, and the ion chamber used for commissioning is available for the measurements made in the water tank.
  - 2. The Intrabeam Water Phantom is used.
- B. Relevant depths of measurement have been determined based on the selections in 1.
  - 1. For example, with the 3.5 cm spherical applicator, at 20 mm depth the dose is less than 10% of the dose at the surface. With a prescription dose of around 18 Gy, the dose at 20 mm is well below relevant dose limits in humans for single fractions [28]. Various depth up to 20 mm can be chosen (e.g. 5, 10 and 20 mm).
  - 2. At very shallow depths (e.g. 2.8 mm described in this study), tissue thickness accuracy is difficult and errors in thickness cause large deviations in measurement. Minimum thickness of 5 mm is recommended unless thinner tissues can be reliably reproduced.
  - 3. By selecting thicknesses in multiples of thinnest tissue (e.g. 5, 10, and 20 mm), a single setting can be used when slicing tissues.
  - 4. A 3D printed holder, as described in the text, is used to hold the OSLDs.

### Full Protocol:

- 1. Scheduling of measurement days
  - a. Measurements will take place over several days and will require reservation of the following at OSU's Carlson College of Veterinary Medicine or Radiation Safety department:
    - i. The Intrabeam and applicators need to be reserved for each measurement day.
    - ii. The Intrabeam Water Phantom needs to be reserved for all ion chamber and calibration measurements for the entire day.
    - iii. A room (like an OR) with little interruption to be reserved for the entire day for each measurement day.
    - iv. Mobile shielding, lead vests, and a survey meter must be obtained/reserved for the day. The return of the survey meter to radiation safety may limit the length of time measurements can be made. These are required for each measurement day.

- v. Access to tissue is dependent upon access to recently euthanized cadavers. Cadavers are not always available, so it is recommended to start collecting tissue three weeks before the planned measurement date. Fresher tissue is desired, so if a new cadaver is available, it is recommended to discard the old tissue. Slicing of the tissue into smaller slabs can be done closer to measurement (e.g. just before CT).
  - vi. Appointment with the CT scanner and a CT technologist for tissue measurements for a 30 minute to 1 hour slot. This appointment should either be the day before the tissue measurement day or early enough in the day to allow for analysis of the images prior to measurement.
  - b. It is recommended to schedule arrival as early as possible (e.g. 8:00 AM) to allow for the maximum measurement time.
  - c. NanoDots can be ordered from Landauer, Inc. with a lead time on the order of a week, but these should be ordered as early as possible. For each applicator, it is recommended that 50 NanoDots are ordered.
2. Water Tank Measurement and NanoDot Calibrations (Estimated time: 1 day per applicator)
- a. The first day of measurement and NanoDot calibrations can be extensive, so it is recommended that only one applicator be used.
  - b. The following items are necessary for water tank measurement:
    - i. Intrabeam system and applicators
    - ii. Intrabeam QA equipment
    - iii. Intrabeam Soft X-Ray ionization chamber
    - iv. Intrabeam calibration files
    - v. Intrabeam Water Phantom
    - vi. 4 L of deionized water -- Likely accessible within the lab
    - vii. Nanodots
    - viii. 3D printed nanoDot holder
    - ix. Forceps for the removal of the NanoDots holder from the Ionization Chamber holder
    - x. Lead vests and mobile shielding
    - xi. Survey Meter
    - xii. Something to organize nanodots after irradiation (e.g. a plastic sleeve with individual labeled pockets or sheets of paper and masking tape)
    - xiii. A cooler and ice to maintain tissue temperature
    - xiv. Rubber Gloves
    - xv. Water equivalent plastic (in kV range) for backscatter in tissue measurements
    - xvi. Laptop to record ion chamber data
    - xvii. Camera
  - c. Water tank measurements with ion chamber

- i. Thoroughly review the *Intrabeam Water Phantom Instructions for Use* and *Landauer Calibrating the microStar* prior to the day of measurement.
  - ii. Once all items have been moved into the reserved room, the Intrabeam must be powered on and QA should be performed per the instructions on the system.
    - 1. The QA process can take a variable amount of time. Be prepared for initial QA to take as much as one hour.
  - iii. After filling the water tank with deionized water, align the Intrabeam XRS to the water tank and place the applicator in the water tank using the recommendations in the *Intrabeam Water Phantom Instructions for Use*.
    - 1. During this initial time with the beam on, with the survey meter, verify that the water tank is well-shielded.
  - iv. Make measurements of dose rate with the ion chamber at several depths including at the surface of the applicator and each depth that NanoDots will be measured. The dose rates should be checked against the original depth dose curve for the applicator. Any deviation greater than 5% should prompt a verification of the setup and additional measurements.
    - 1. Make sure to factor in the thickness of both the ion chamber holder (printed on the surface of the holder) and the depth to the point of measurement when translating the Intrabeam.
    - 2. Set a prescription dose of 99 Gy to the surface of the applicator. By pausing the treatment delivery between measurements, several depths can be measured without entering additional prescriptions or completing additional QAs.
- d. Water tank measurements with NanoDots for calibration
- i. Because of the NanoDots high energy dependence in the kV range and the rapidly changing beam quality of the Intrabeam's spectrum with depth, it is recommended (at least initially) to make separate calibrations for each depth to be measured.
  - ii. The *microStar Calibration and Usage Instructions* recommends 7 dose levels for calibration and 3 NanoDots per dose level. In the configuration described here, this would require 21 separate Intrabeam treatments that would take between 1 and 20 minutes. This amount of time would not be feasible, so it is recommended that 5 separate dose levels from 1 Gy to 20 Gy (prescribed to the surface of the applicator) be used to create a non-linear calibration curve. This will cover the entire prescription dose range. It is also recommended to irradiate two NanoDots at each dose level. This process is estimated to take approximately 2 hours per depth. At greater depths, the dose

to the NanoDots is lower, so a linear calibration curve can be used. A table in Appendix B lays out the measurements needed for a calibration.

- iii. Additional NanoDots should be irradiated to the exact prescription dose.
- iv. For each treatment delivery, it is recommended that an additional 0.02-0.03 Gy be added to the prescription, so that treatment can be stopped before completion, but the total intended prescribed dose is delivered (see figure below). This process will minimize the number of QAs that are normally required after every 3 completed treatments; however, there will still be required QAs after extensive periods of treatment.

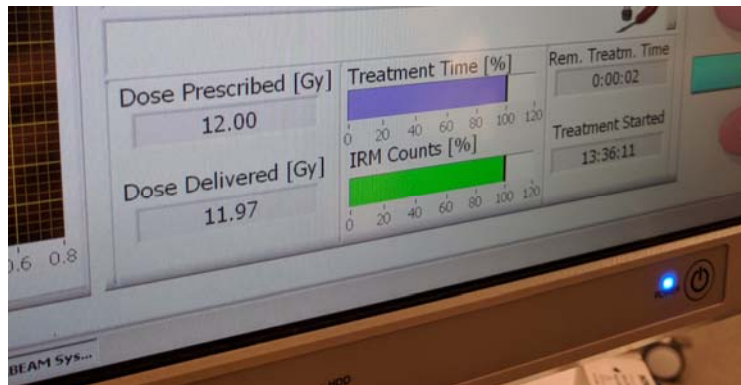


**Figure 23. Early Treatment Termination**

- v. While irradiating make sure to cover all NanoDots with lead, or store them outside the room to prevent additional radiation from reaching them.
- vi. When placing the NanoDots in the 3D printed NanoDot holder, make sure that they are all placed in the same orientation (see figure below).



**Figure 24. nanoDot Orientation in Holder**

- vii. The entire process of ion chamber measurements and NanoDot calibrations are estimated to take an entire day for a single applicator.
- viii. A table is provided in Appendix B that can be used as a template for data collection during measurement.

- ix. After the calibrations have been completed with the microStar reader at OHSU's Department of Radiation Medicine using the procedure in *microStar Calibration and Usage*, the calibrations can be analyzed to determine if calibrations at additional depths would be useful or if interpolation between calibration curves could be used.
3. Tissue harvesting (Estimated lead time: 3 weeks ahead of measurement date)
    - a. As stated above, tissue harvesting can require the longest lead time, so it should be requested at least three weeks prior to the measurement date.
    - b. For the case of muscle tissue, a sample of relatively uniform 4 cm thickness and 5 cm x 5 cm cross section should be requested. If a 4 cm tissue sample cannot be obtained, two samples of at least 2 cm would be appropriate.
    - c. The tissue harvesting will be completed by a surgeon at OSU's College of Veterinary Medicine using a meat slicer with adjustable thickness.
    - d. Using the assumption in B.3., and minimum slice thickness of 5 mm, the tissue should be sliced into multiple 5 mm slices. By making all of the slices at the same thickness, the setting of the slicer can be held constant. This will make the slices more consistent.

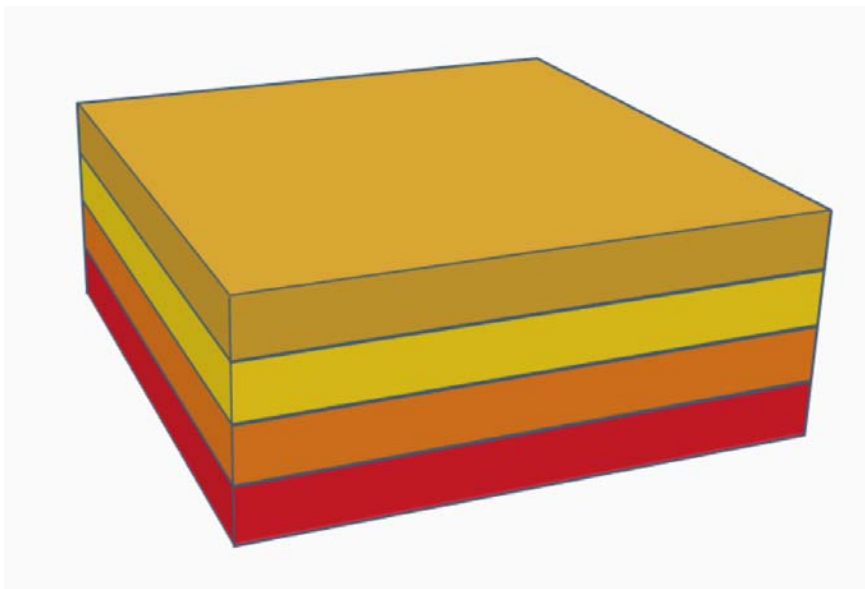


**Figure 25. Tissue Slab Diagram**

**The tissue is broken into identical 5 mm slabs. The dimensions on each side are 50 mm x 50 mm.**

- e. For both of these methods, the tissue will be frozen for a period of 30 minutes to 1 hour to aid in slicing.
  - f. Each sample should be labeled so that it can be distinguished during imaging and measurement.
  - g. The samples should be wrapped in saline-soaked gauze and kept on ice to prevent desiccation.
4. CT of Tissue (Estimated time: 30 minutes to 1 hour)

- a. The CT of the tissue should be done prior to the planned measurement day or should be early enough to allow analysis of the tissue thicknesses.
  - b. The CT should be taken with a flat surface, such as the water equivalent plastic placed on top of the curved couch.
  - c. Plenty of pictures of the tissue should be taken to verify orientation. Any identifying features (e.g. epimysium or “silver skin”) should be documented as it will aid in orientation during NanoDot placement and irradiation. Marks distinguishing the tissue should be visible in these photos.
  - d. Analyze the images in a DICOM viewer like K-PACS to determine the actual thickness and optimal nanoDot placement. It is suggested to use Window and Level settings of 400 and 0, respectively.
5. Tissue measurements with NanoDots
- a. Extra attention should be paid to shielding during tissue measurements. Lead vests and mobile radiation shields should be in place. Any NanoDots not being irradiated should be moved outside the room.
  - b. Measurement should take place with the tissue sample placed on water equivalent plastic. Plastic wrap placed over the water equivalent plastic will prevent contamination of the plastic.
  - c. If the solid water has a cutout available for an ion chamber, it can be filled with bolus to create a well-defined area for repeatable placement (see figure below).

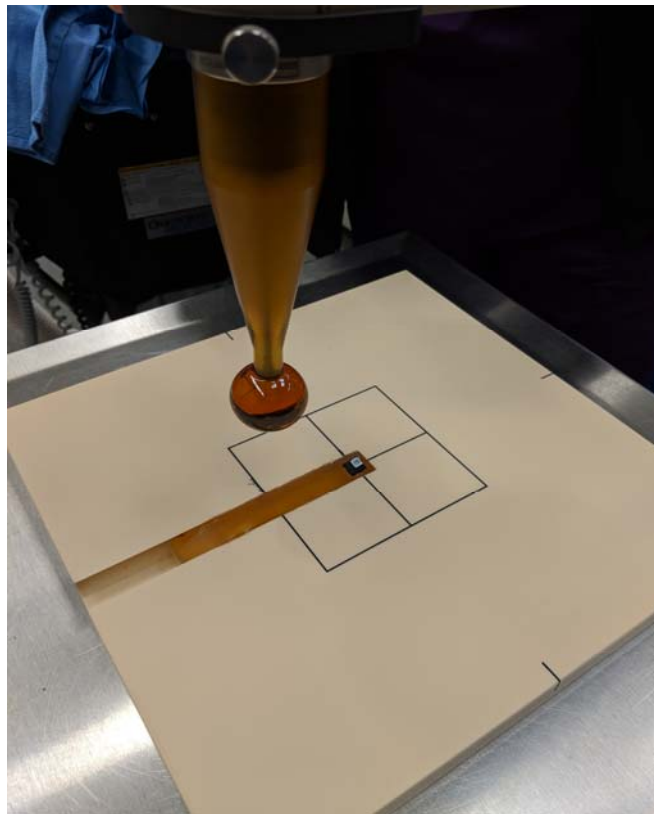


**Figure 26. nanoDot Placement on Bolus**

- d. When placing the tissue, make sure to pay careful attention so that the area covering the NanoDot is the same area that was measured with the CT. The orientation of the tissue should be the same as the CT, as well.
- e. The tissue should be placed on the NanoDot carefully to ensure that it does not slide.
- f. The applicator should be placed on the tissue with care taken so that it is orthogonal to the tissue with only enough pressure on the tissue to establish contact across the bottom of the applicator. This will prevent compression caused by the pressure on the tissue (see figure below).

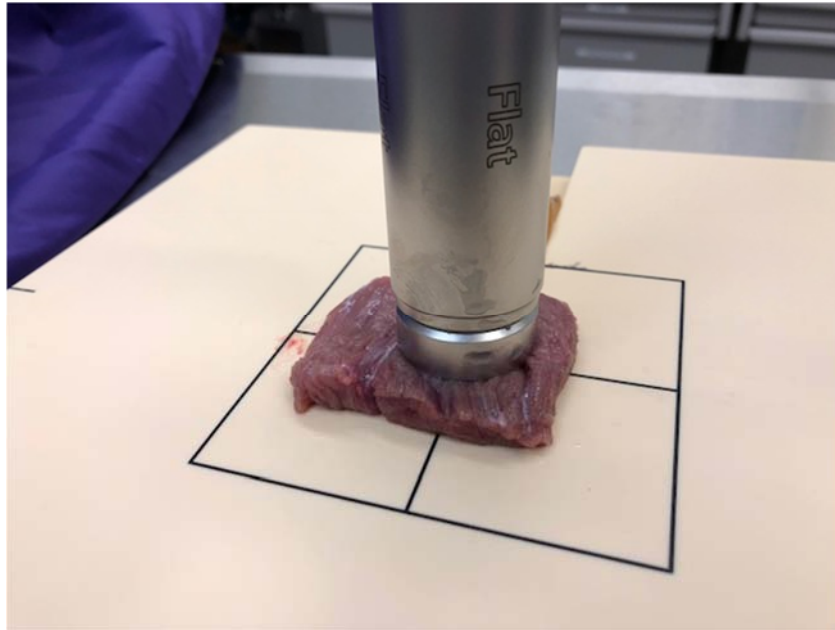


**Figure 27. Applicator Placement on Tissue**

- g. Especially in thinner samples, there can be some tissue heating during the course of a treatment. It is suggested that tissue samples are cycled and placed back in the cooler between treatments.
- h. For measurements requiring greater depth, the tissue samples should be stacked to reach the desired height. The orientation and order of the tissues should be noted and held consistent.
- i. It is recommended that at least two NanoDots be irradiated to the clinical prescription dose for each tissue thickness. With additional time, additional NanoDots can be irradiated to the prescription dose or other relevant doses.
- j. A table has been provided in Appendix B to aid in data collection when measuring in tissue.
- k. When reading the nanoDots with the microStar, ensure to select the calibration corresponding to the measurement depth of the NanoDot.

## B. Sample Data Tables

Table 6 shows a sample data table that lays out the number of nanoDots required for each calibration. The table is organized such that the depth and the PDD can be entered manually and the dose to each nanoDot is calculated. For each dose level, the nanoDots are labeled with a number and the letters *A* and *B* corresponding to the two nanoDots used at each dose level for calibration. The prescription to the applicator can be adjusted if higher doses are necessary. This table should be used in conjunction with the calibration tool in the microStar software to create the calibration curves. The table is provided with a 5 mm depth and 0.5 PDD for example purposes only.

**Table 6. Sample Data Table for nanoDot Calibrations**

| Depth (mm): 5 |                                 | PDD @ Depth: 0.5  |        |
|---------------|---------------------------------|-------------------|--------|
| nanoDot       | Prescription to Applicator (Gy) | Dose @ Depth (Gy) | Counts |
| 1A            | 0                               | 0                 |        |
| 1B            | 0                               | 0                 |        |
| 2A            | 5                               | 2.5               |        |
| 2B            | 5                               | 2.5               |        |
| 3A            | 10                              | 5                 |        |
| 3B            | 10                              | 5                 |        |
| 4A            | 15                              | 7.5               |        |
| 4B            | 15                              | 7.5               |        |
| 5A            | 20                              | 10                |        |
| 5B            | 20                              | 10                |        |

Table 7 shows a sample table that can be used for data collection for ion chamber and nanoDot measurements in the water tank. The applicators and depths should be known ahead of time. After measuring the charge collected in one minute, the dose rate is found based off of equation 2. The treatment is based on the time on the console when irradiating the nanoDot. The dose delivered to the nanoDot will be the dose rate multiplied by the treatment time.

